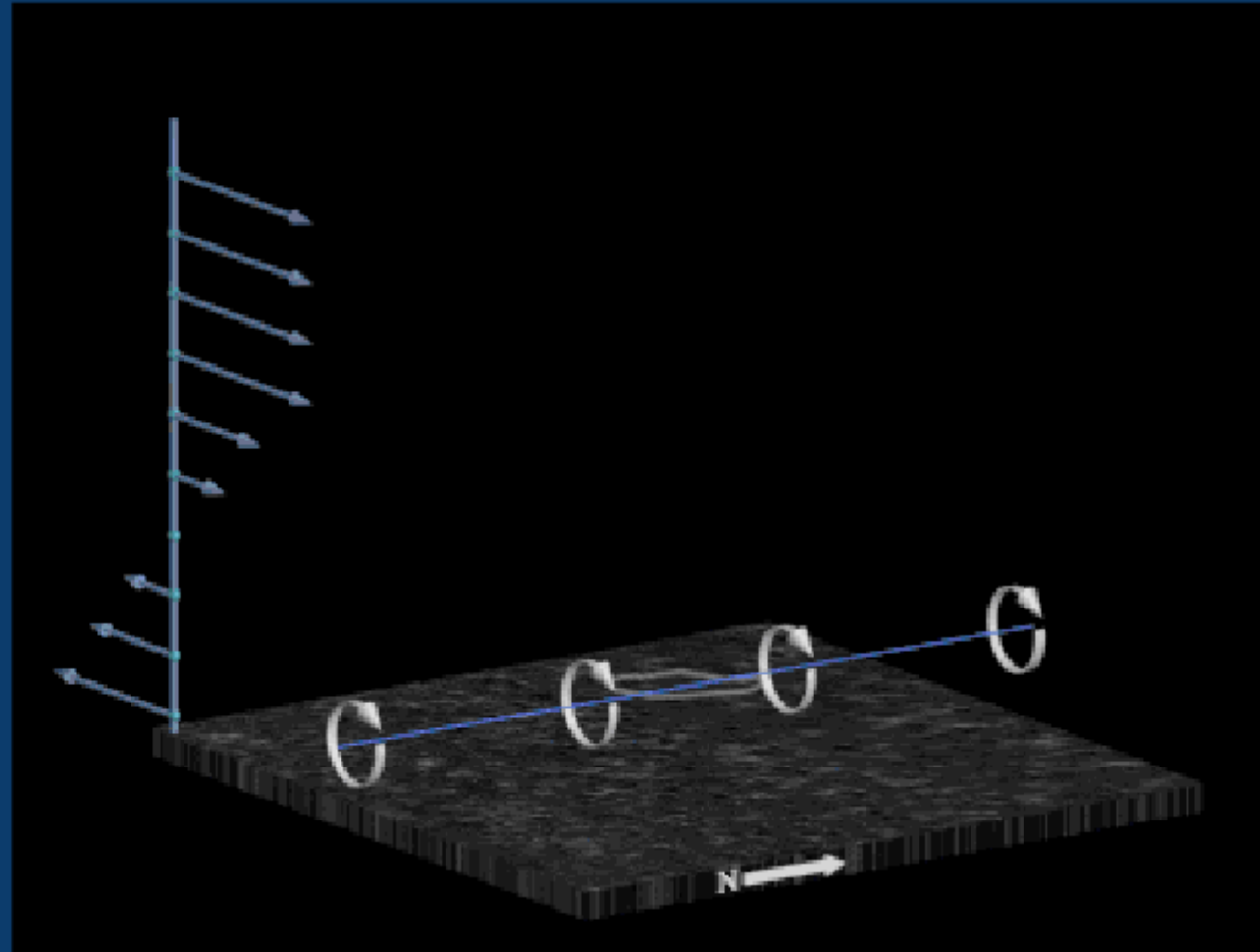
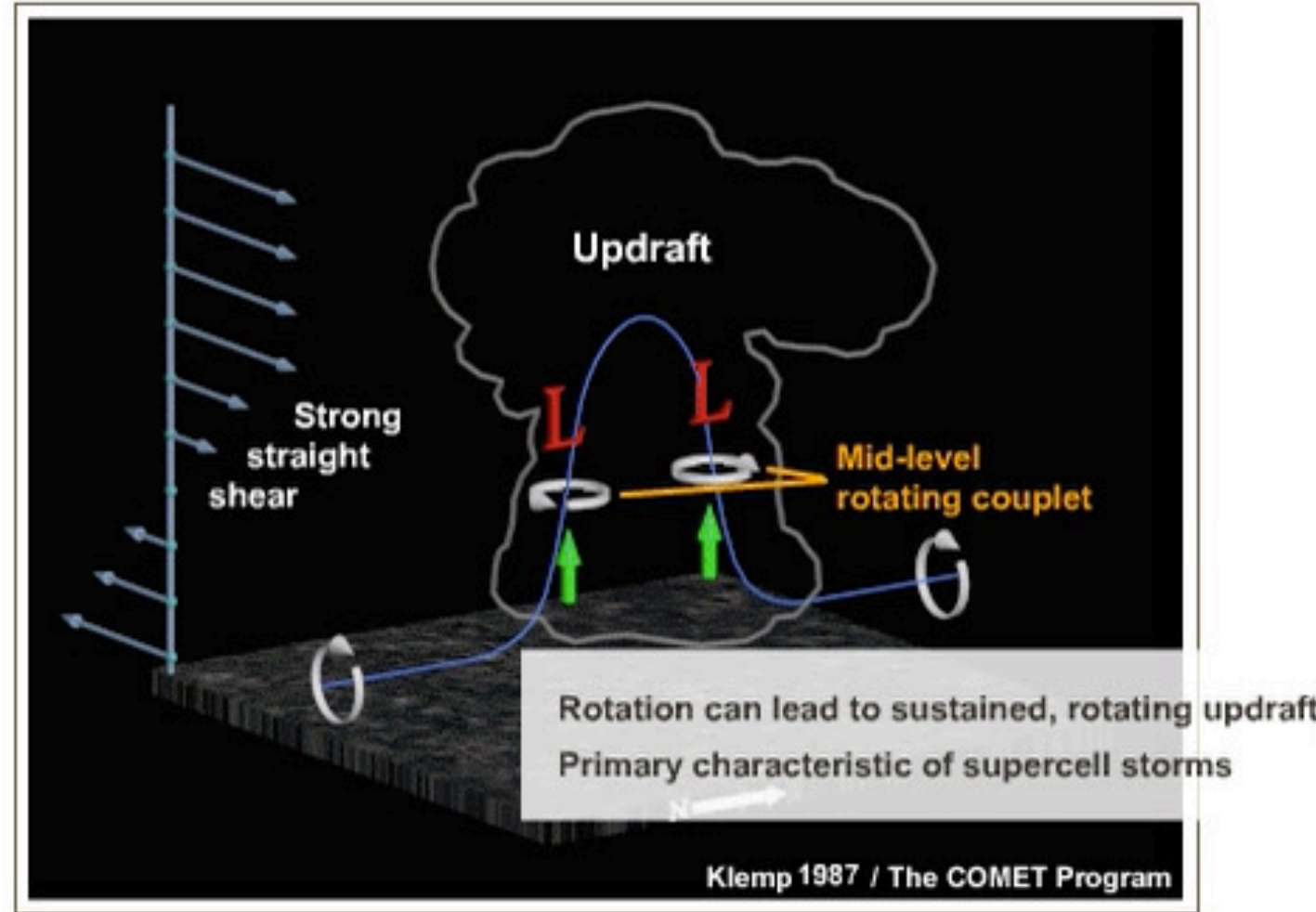


Tilting of horizontal vortex line



Klemp, 1987/The COMET Program





上节课回顾

垂直涡度倾向方程 (Boussinesq近似, 忽略摩擦力和科氏力项)

$$\frac{d\zeta}{dt} = \xi \frac{\partial w}{\partial x} + \eta \frac{\partial w}{\partial y} + \zeta \frac{\partial w}{\partial z}$$

$$\frac{\partial \zeta}{\partial t} = -\vec{v} \cdot \nabla \zeta + \vec{\omega} \cdot \nabla w$$

$$= -u \frac{\partial \zeta}{\partial x} - v \frac{\partial \zeta}{\partial y} - w \frac{\partial \zeta}{\partial z} + \xi \frac{\partial w}{\partial x} + \eta \frac{\partial w}{\partial y} + \zeta \frac{\partial w}{\partial z}$$

$$= -u \frac{\partial \zeta}{\partial x} - v \frac{\partial \zeta}{\partial y} - w \frac{\partial \zeta}{\partial z}$$

平流项 (Advection)

$$+ \left(\frac{\partial w}{\partial y} - \frac{\partial v}{\partial z} \right) \frac{\partial w}{\partial x} + \left(\frac{\partial u}{\partial z} - \frac{\partial w}{\partial x} \right) \frac{\partial w}{\partial y}$$

倾斜项 (Tilting)

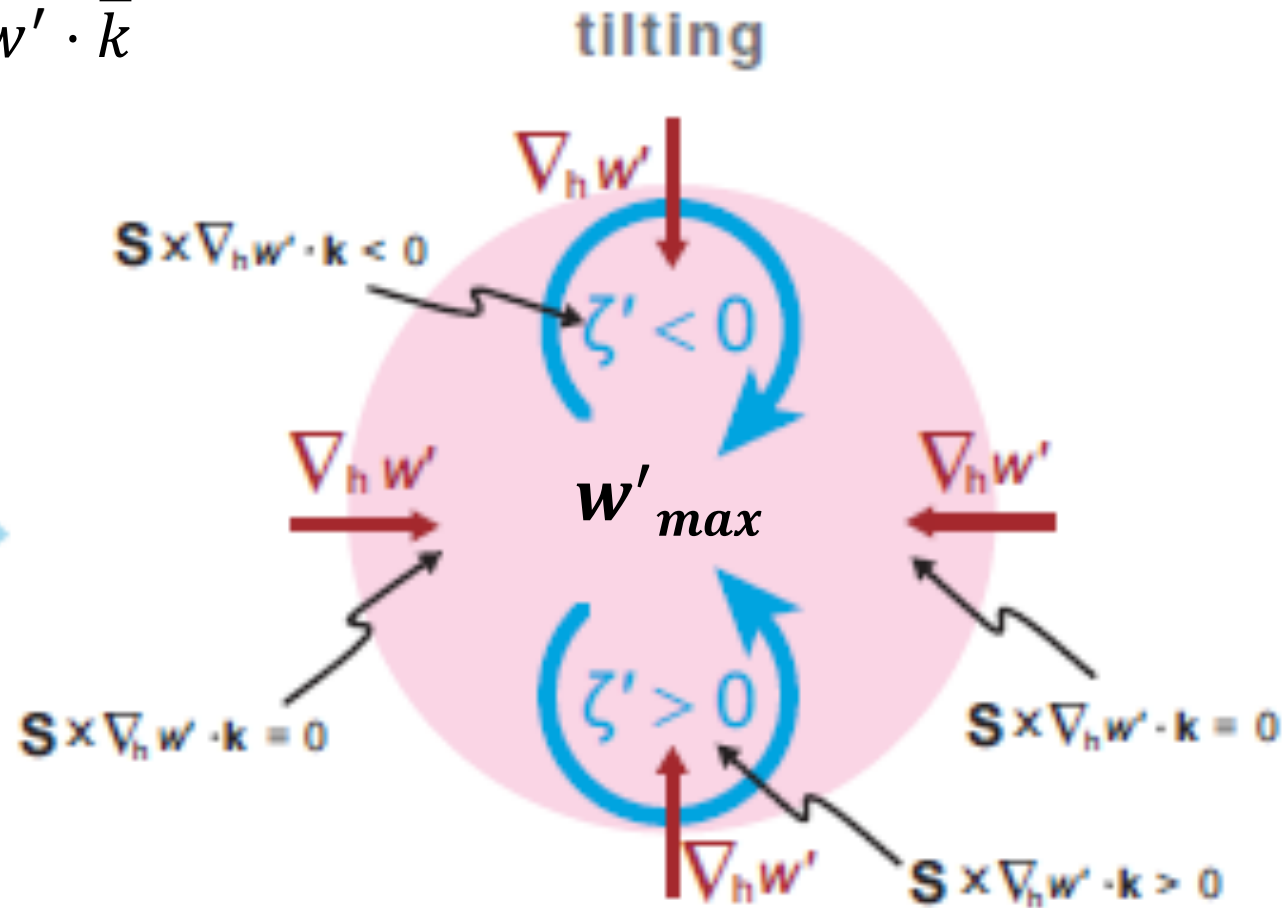
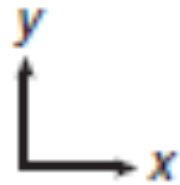
$$+ \left(\frac{\partial v}{\partial x} - \frac{\partial u}{\partial y} \right) \frac{\partial w}{\partial z}$$

拉伸项 (Stretching)

①

$$\left(\frac{\partial \zeta'}{\partial t}\right)_{sr} = -(\vec{v} - \vec{c}) \cdot \nabla \zeta' + \vec{s} \times \nabla w' \cdot \vec{k}$$

$$\left(\frac{\partial \zeta'}{\partial t}\right)_{sr} \propto \vec{s} \times \nabla w' \cdot \vec{k}$$



在垂直于切变矢量的方向上垂直最大抬升的两侧产生两个对称的反向涡旋，切变矢量的左边为负涡度，右边为正涡度

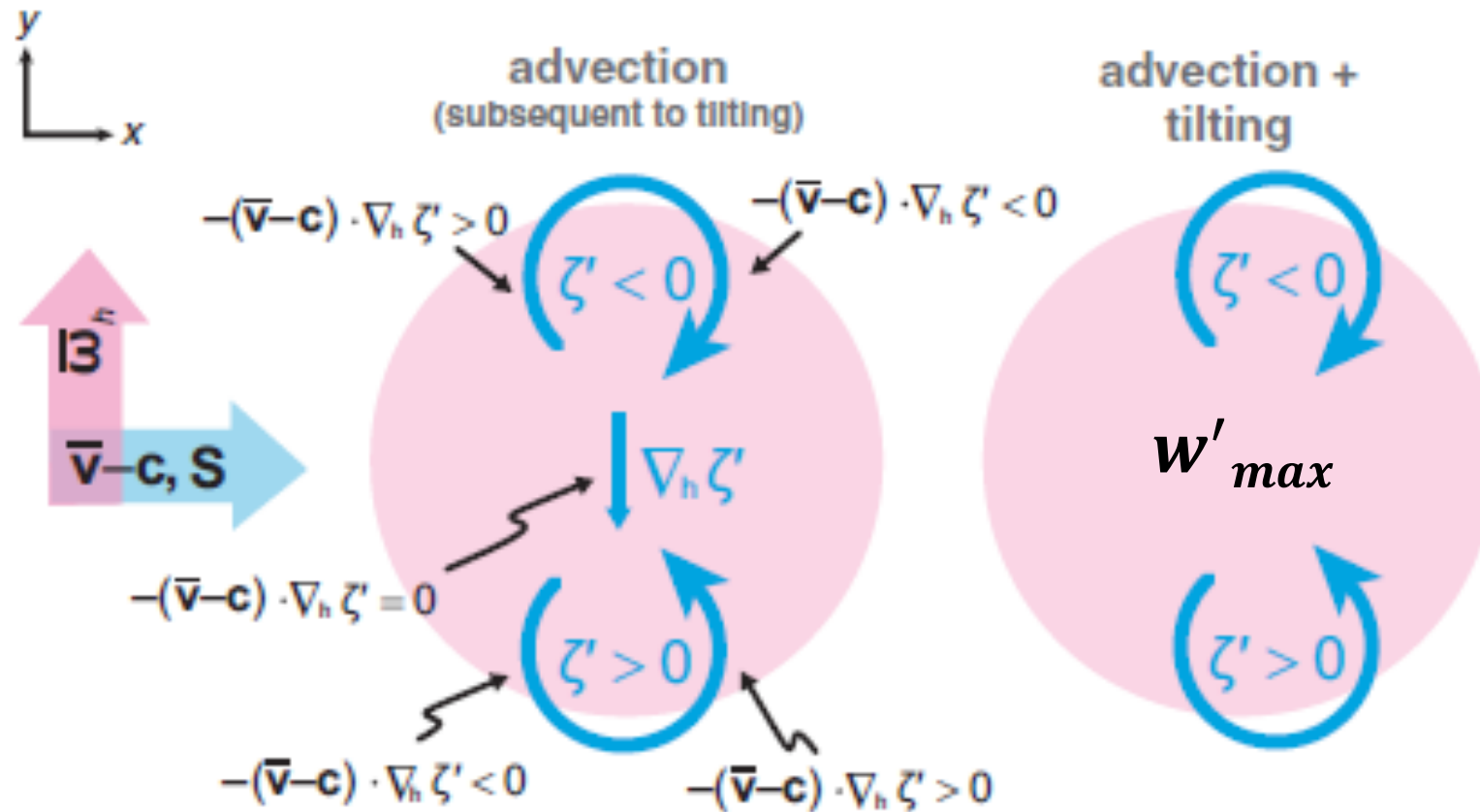
$$\left(\frac{\partial \zeta'}{\partial t}\right)_{sr} = -(\vec{v} - \vec{c}) \cdot \nabla \zeta' + \vec{s} \times \nabla w' \cdot \vec{k}$$



$$\left(\frac{\partial \zeta'}{\partial t}\right)_{sr} \propto -(\vec{v} - \vec{c}) \cdot \nabla \zeta'$$

a. Crosswise vorticity: Storm relative wind与水平涡度垂直

$$(\vec{v} - \vec{c}) \perp \vec{\omega}_h$$



涡度对被向下切变方向平流

$$\left(\frac{\partial \zeta'}{\partial t}\right)_{SR} \propto -(\bar{\mathbf{v}} - \bar{\mathbf{c}}) \cdot \nabla \zeta'$$

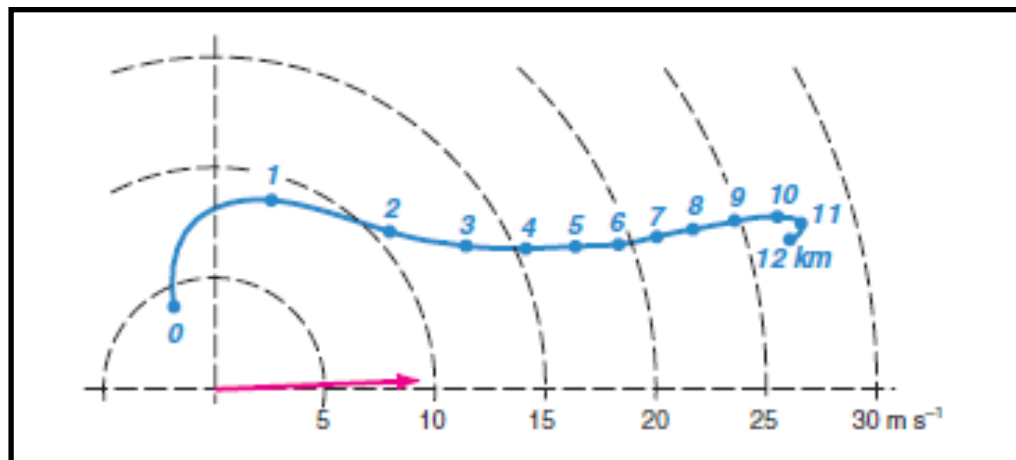


b. Streamwise vorticity: Storm relative wind与水平涡度平行

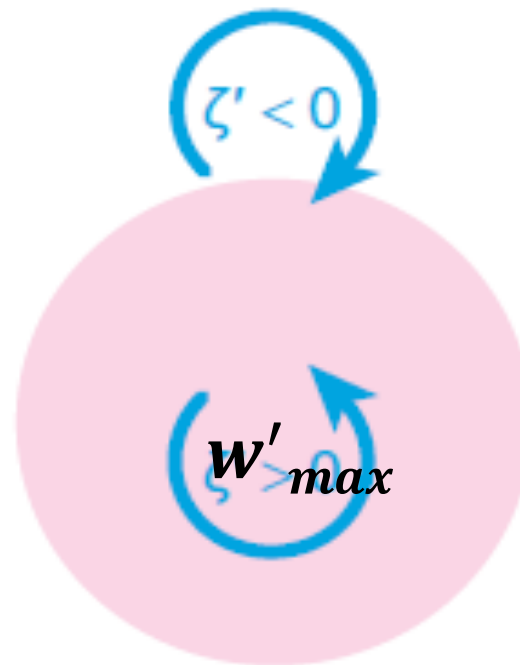
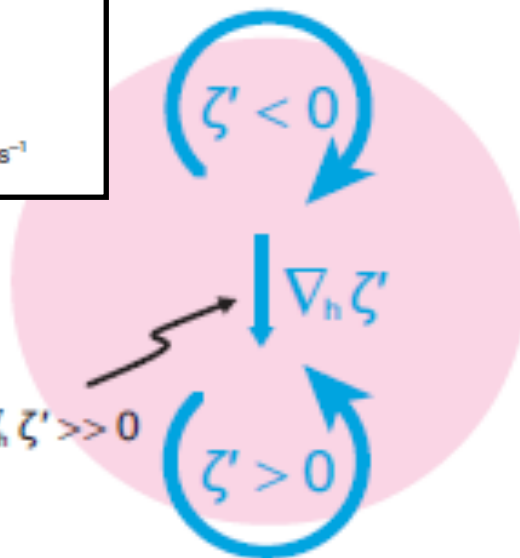
$$(\bar{\mathbf{v}} - \bar{\mathbf{c}}) \parallel \bar{\boldsymbol{\omega}}_h$$

advection + tilting

advection
(subsequent to tilting)



$$-(\bar{\mathbf{v}} - \bar{\mathbf{c}}) \cdot \nabla_h \zeta' \gg 0$$



平流幅度较Crosswise情况大。由于 $\nabla \zeta'$ 较大，再经上升气流拉伸，正涡旋比crosswise的强。Updraft与 $\zeta' > 0$ 的重合程度取决于水平涡度在storm relative wind 方向上的分量大小。

螺旋度：Helicity

表征流体运动矢量与其涡度矢量的重合程度

$$H = \bar{\mathbf{v}} \cdot \bar{\boldsymbol{\omega}}$$

$$= u \left(\frac{\partial w}{\partial y} - \frac{\partial v}{\partial z} \right) + v \left(\frac{\partial u}{\partial z} - \frac{\partial w}{\partial x} \right) + w \left(\frac{\partial v}{\partial x} - \frac{\partial u}{\partial y} \right)$$

假定w为0

$$H = -u \frac{\partial v}{\partial z} + v \frac{\partial u}{\partial z} = \bar{\mathbf{v}} \cdot \bar{\mathbf{k}} \times \frac{\partial \bar{\mathbf{v}}}{\partial z} = -\bar{\mathbf{k}} \cdot \left(\bar{\mathbf{v}} \times \frac{\partial \bar{\mathbf{v}}}{\partial z} \right)$$

$$= -\bar{\mathbf{k}} \cdot (\bar{\mathbf{v}} \times \bar{\mathbf{s}})$$

Storm relative helicity (SRH)

$$\begin{aligned} \text{SRH} &= \int_0^d (\vec{v} - \vec{c}) \cdot \vec{\omega}_h dz = \int_0^d |\vec{v} - \vec{c}| \omega_s dz \\ &= \int_0^d (\vec{v} - \vec{c}) \cdot \vec{k} \times \vec{s} dz = - \int_0^d \vec{k} \cdot (\vec{v} - \vec{c}) \times \vec{s} dz \end{aligned}$$

Estimation on a hodograph

$$\text{SRH} = 2 \text{ GreenArea}$$

可用于预报Supercell的可能性

0-3 km SRH > 150 m²s⁻²

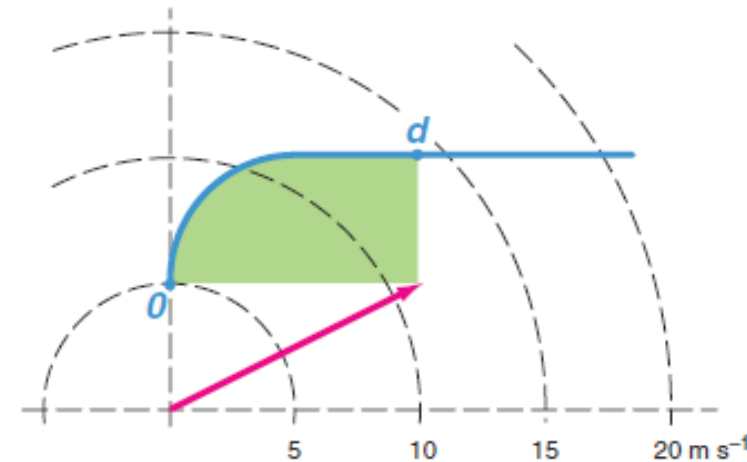
超级单体

0-3 km SRH > 400 m²s⁻²

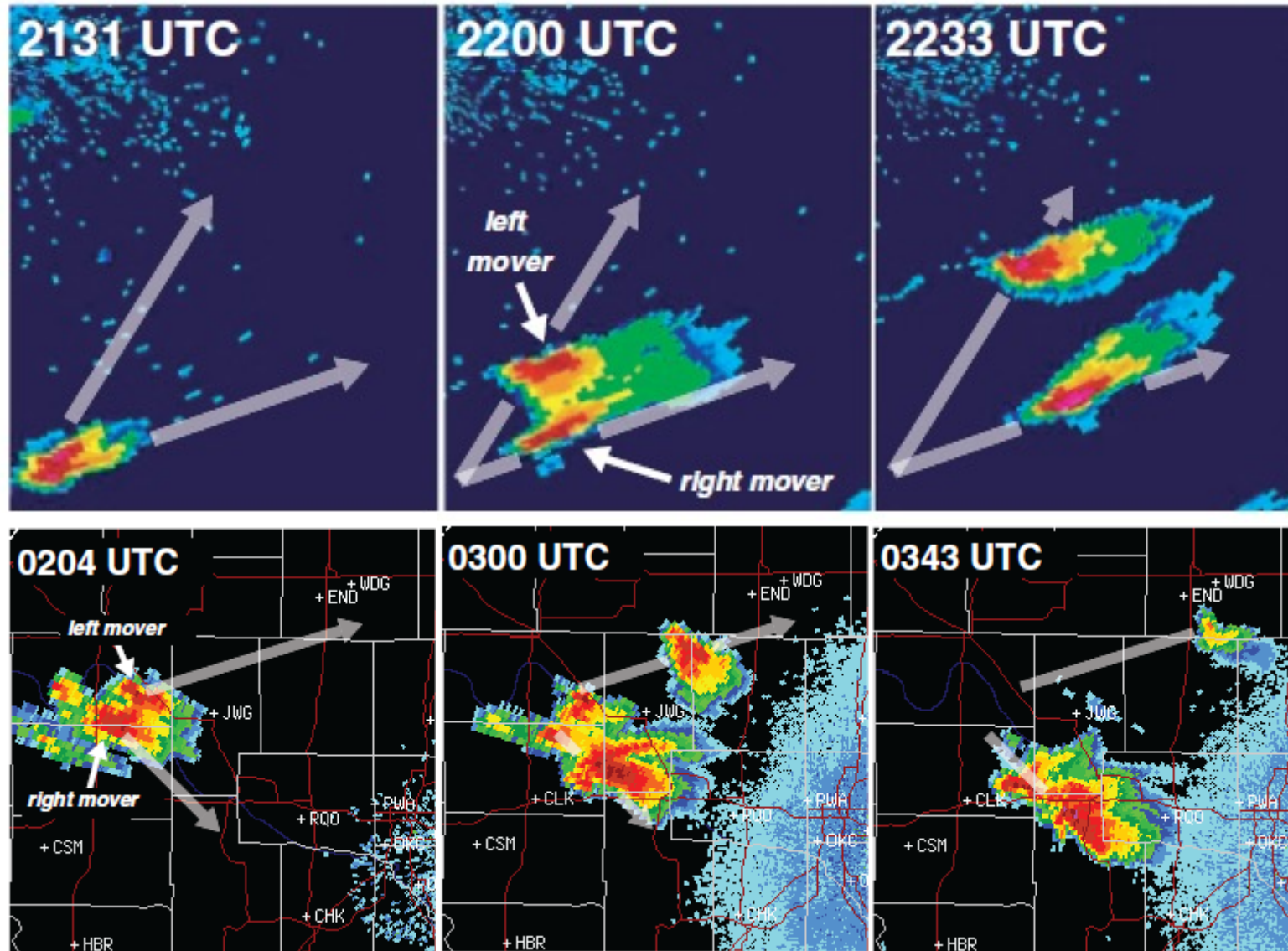
龙卷和超级单体爆发

0-1 km SRH

可用于区分tornadic 和nontornadic supercells.



(5) 超级单体的传播



1) 动力扰动气压

$$\nabla^2 p' = -\rho_0 \nabla \cdot (\vec{v} \cdot \nabla \vec{v}) + \rho_0 \frac{\partial B}{\partial z} - \rho_0 f \nabla \cdot (\vec{k} \times \vec{v})$$

$$p_D' \propto e_{ij}^2 - \frac{1}{2} |\vec{\omega}|^2$$

$$p_D' \propto e_{ij}'^2 - \frac{1}{2} |\vec{\omega}'|^2 + 2 \left(\frac{\partial w'}{\partial x} \frac{\partial \bar{u}}{\partial z} + \frac{\partial w'}{\partial y} \frac{\partial \bar{v}}{\partial z} \right)$$

非线性动力
扰动气压

线性动力扰动气压

1) 动力扰动气压

$$p_D' \propto e_{ij}'^2 - \frac{1}{2} |\vec{\omega}'|^2 + 2 \left(\frac{\partial w'}{\partial x} \frac{\partial \bar{u}}{\partial z} + \frac{\partial w'}{\partial y} \frac{\partial \bar{v}}{\partial z} \right)$$



非线性动力
扰动气压

线性动力扰动气压

$$p' \propto \left[\left(\frac{\partial u'}{\partial x} \right)^2 + \left(\frac{\partial v'}{\partial y} \right)^2 + \left(\frac{\partial w'}{\partial z} \right)^2 \right] \quad \text{变形}$$

$$+ 2 \left[\frac{\partial v'}{\partial x} \frac{\partial u'}{\partial y} + \frac{\partial w'}{\partial x} \frac{\partial u'}{\partial z} + \frac{\partial w'}{\partial y} \frac{\partial v'}{\partial z} \right] \quad \text{旋转}$$

$$+ 2 \vec{s} \cdot \nabla_h w' \quad \text{线性动力扰动气压}$$

$$- \frac{\partial B}{\partial z} \quad \text{浮力项}$$

对于**高速垂直旋转流**内部，变形可以忽略，水平涡度可以忽略

忽略变形：
$$\frac{\partial v'}{\partial x} + \frac{\partial u'}{\partial y} = \frac{\partial w'}{\partial y} + \frac{\partial v'}{\partial z} = \frac{\partial w'}{\partial x} + \frac{\partial u'}{\partial z} = 0$$

deformation

$$E_{ij} = \frac{1}{2} (\partial_j v_i + \partial_i v_j)$$

$\Rightarrow \frac{\partial v'}{\partial x} = -\frac{\partial u'}{\partial y}, \frac{\partial w'}{\partial y} = -\frac{\partial v'}{\partial z}, \frac{\partial w'}{\partial x} = -\frac{\partial u'}{\partial z}$ ①

忽略水平涡度：
$$\frac{\partial w'}{\partial y} - \frac{\partial v'}{\partial z} = \frac{\partial u'}{\partial z} - \frac{\partial w'}{\partial x} = 0$$

$\Rightarrow \frac{\partial w'}{\partial y} = \frac{\partial v'}{\partial z}, \frac{\partial u'}{\partial z} = \frac{\partial w'}{\partial x}$ ②

由 ① 和 ② 可得：
$$\frac{\partial w'}{\partial y} = \frac{\partial v'}{\partial z} = \frac{\partial u'}{\partial z} = \frac{\partial w'}{\partial x} = 0$$

$$\frac{\partial w'}{\partial y} = \frac{\partial v'}{\partial z} = \frac{\partial u'}{\partial z} = \frac{\partial w'}{\partial x} = 0$$

$$\frac{\partial v'}{\partial x} = -\frac{\partial u'}{\partial y},$$

于是

$$2 \left[\frac{\partial v'}{\partial x} \frac{\partial u'}{\partial y} + \cancel{\frac{\partial w'}{\partial x} \frac{\partial u'}{\partial z}} + \cancel{\frac{\partial w'}{\partial y} \frac{\partial v'}{\partial z}} \right] \quad \text{简化为: } 2 \frac{\partial v'}{\partial x} \frac{\partial u'}{\partial y}$$

与 ζ' 的关系?

$$2 \frac{\partial v'}{\partial x} \frac{\partial u'}{\partial y} = -\frac{1}{2} \left[-\frac{\partial v'}{\partial x} \frac{\partial u'}{\partial y} - 2 \frac{\partial v'}{\partial x} \frac{\partial u'}{\partial y} - \frac{\partial v'}{\partial x} \frac{\partial u'}{\partial y} \right]$$

$$= -\frac{1}{2} \left[\frac{\partial v'}{\partial x} \frac{\partial v'}{\partial x} - 2 \frac{\partial v'}{\partial x} \frac{\partial u'}{\partial y} + \frac{\partial u'}{\partial y} \frac{\partial u'}{\partial y} \right]$$

$$= -\frac{1}{2} \left[\frac{\partial v'}{\partial x} - \frac{\partial u'}{\partial y} \right]^2 = -\frac{1}{2} [\zeta']^2$$

于是

$$p' \propto \left[\left(\frac{\partial u'}{\partial x} \right)^2 + \left(\frac{\partial v'}{\partial y} \right)^2 + \left(\frac{\partial w'}{\partial z} \right)^2 \right] \left[-\frac{1}{2} [\zeta']^2 + 2\vec{s} \cdot \nabla_h w' \right] - \frac{\partial B}{\partial z}$$

超级单体情形

动力强迫 $-\alpha \frac{\partial p'_D}{\partial z}$ 对垂直加速度的贡献与浮力强迫 $-\alpha \frac{\partial p'_b}{\partial z} + B$ 同量级，动力强迫是把负浮力空气抬升到LFC的主要机制。

$$\frac{dw'}{dt} = -\alpha \frac{\partial p'}{\partial z} + B \quad \text{可以简化为} \quad \frac{dw'}{dt} \propto -\frac{\partial p'_D}{\partial z}$$

同时，由于超级单体里变形较小，可以得到

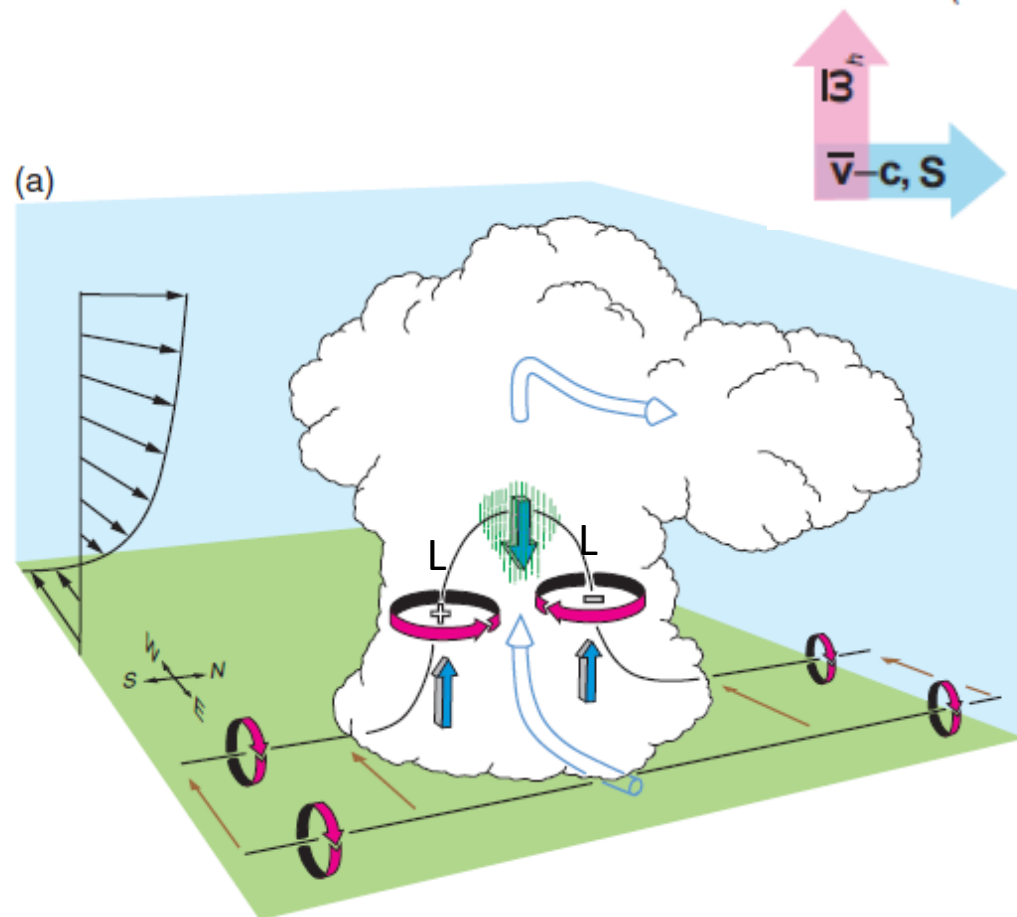
$$\frac{dw'}{dt} \propto \frac{1}{2} \frac{\partial [\zeta']^2}{\partial z} - 2 \frac{\partial}{\partial z} (\vec{s} \cdot \nabla_h w')$$

2) 非线性动力强迫 $-\frac{1}{2}[\zeta']^2$

该项在超级单体发展早期（风暴开始后的**30-60min**）比较重要。

a. 环境为 **crosswise vorticity**，出现**单体分裂**，可多次发生。

- 水平涡管被局地垂直抬升，在中层形成两个垂直涡度中心；
- 非线性动力强迫在两个涡度中心产生低压扰动；
- 在两个涡旋中心形成向上的扰动气压梯度力；
- 原风暴下沉气流进一步使风暴分裂为二（Left mover 和 right mover）。



Nonlinear Contribution to Dynamic Pressure Perturbations

crosswise vorticity

(w' and ζ' uncorrelated)

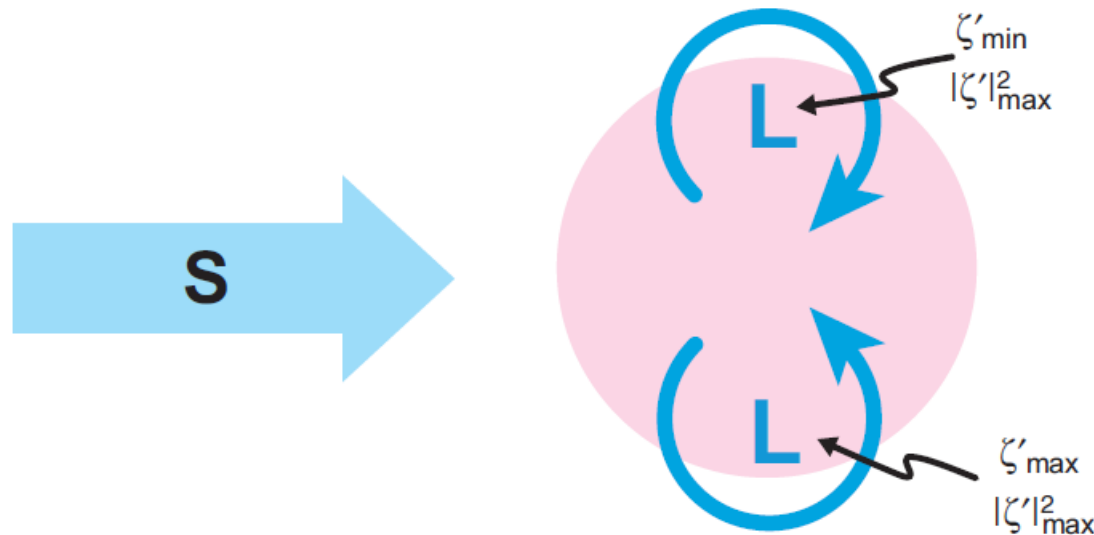
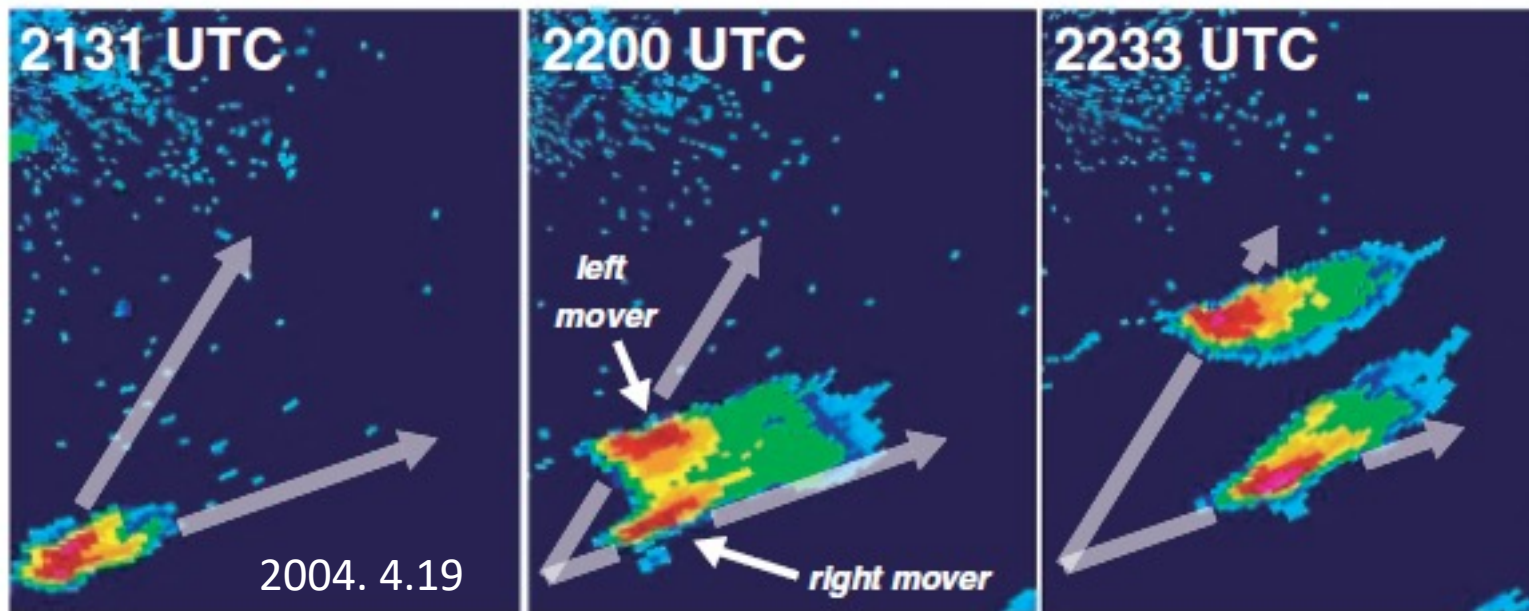


Figure 8.36 Schematic horizontal cross-sections through the midlevel updraft (pink) of a supercell showing the locations of vorticity centers and pressure minima for the cases of purely crosswise vorticity and purely streamwise vorticity. When the vorticity ingested by the updraft is purely crosswise, the $-\frac{1}{2}\zeta'^2$ term in the diagnostic pressure equation leads to an upward-directed dynamic vertical pressure gradient force on the storm flanks below the level of maximum $|\zeta'|$ and minimum p' . In the limit of purely streamwise vorticity being ingested by the updraft, the ζ' and w' fields are approximately in phase; thus, the $-\frac{1}{2}\zeta'^2$ term cannot lead to a significant off-axis, upward-directed, dynamic vertical pressure gradient force.

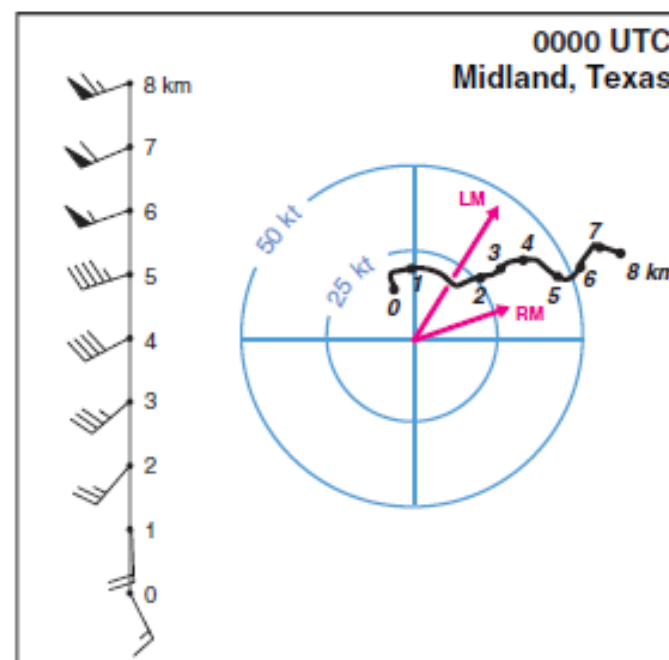
风暴分裂举例



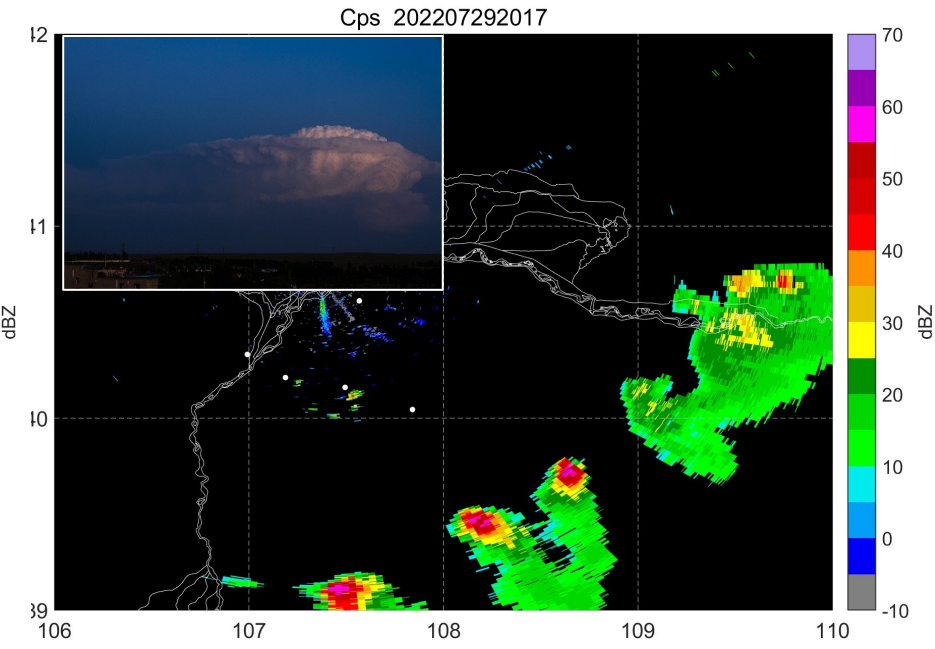
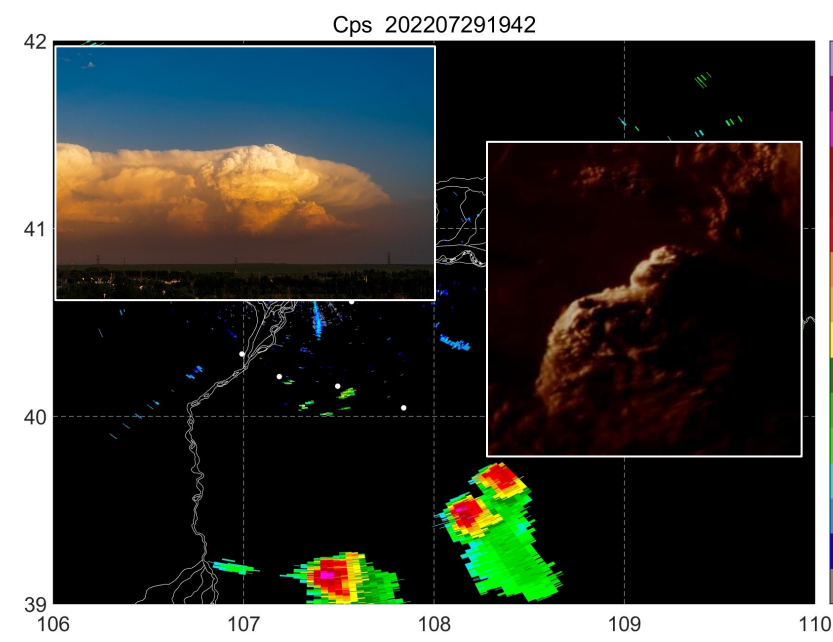
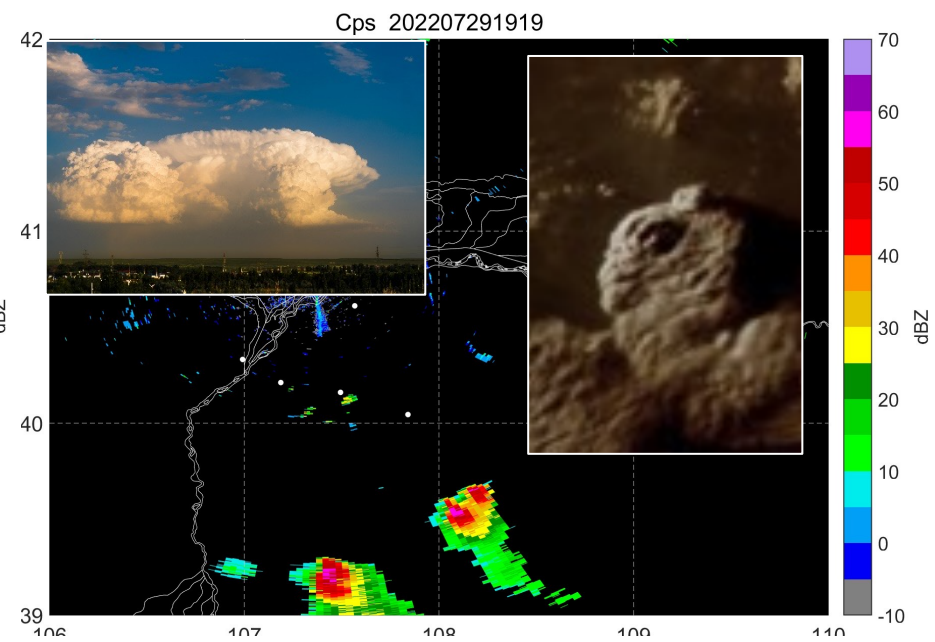
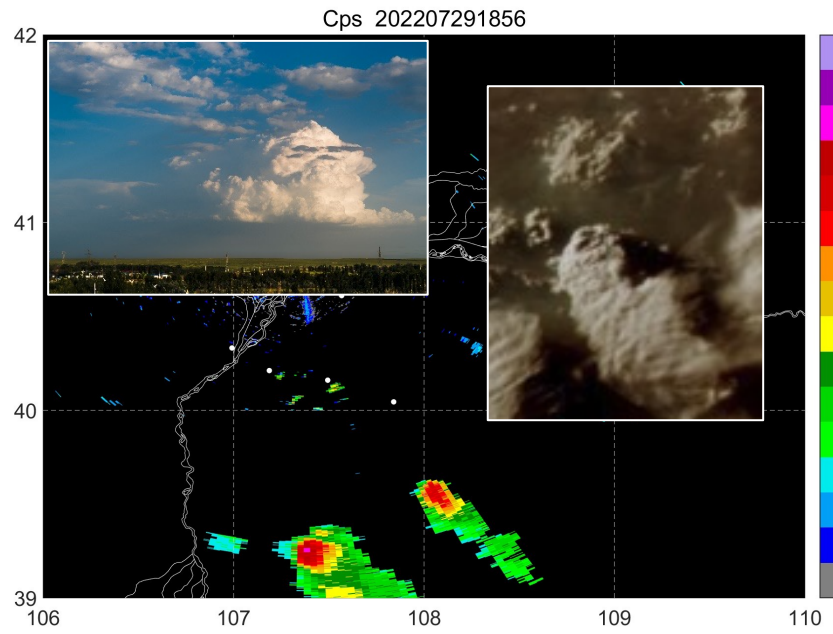


分裂的风暴分别移向深层平均切变矢量的左右两侧

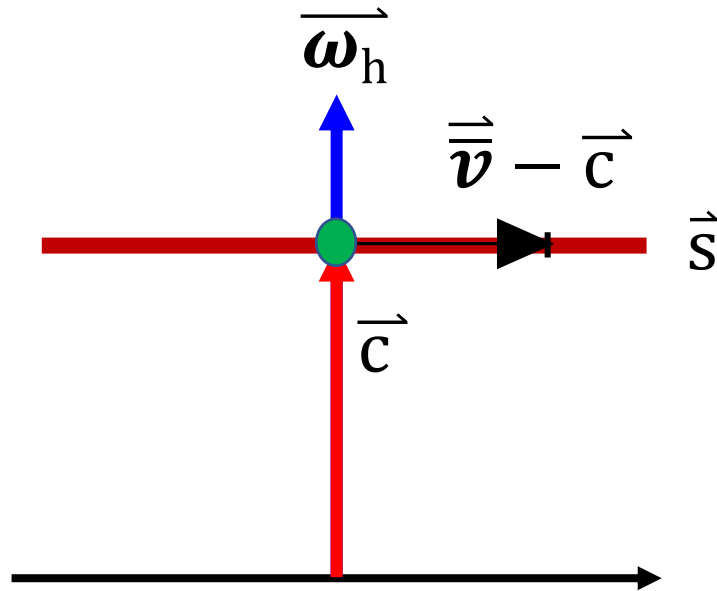
多数情况下，深层切变的方向与深层平均风的方向一致。



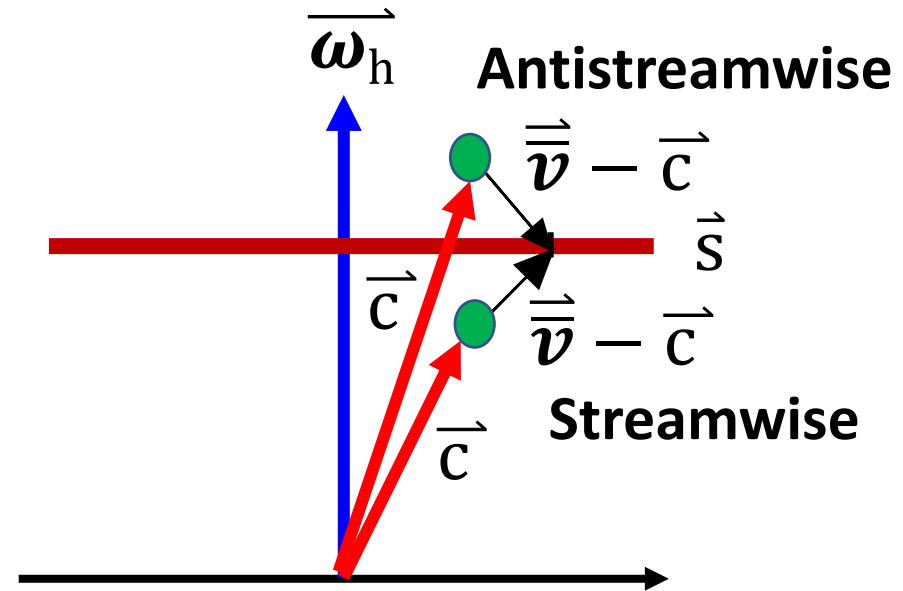




以左移和右移风暴为参考系，其各自的storm relative wind就有了antistream wise和streamwise分量。

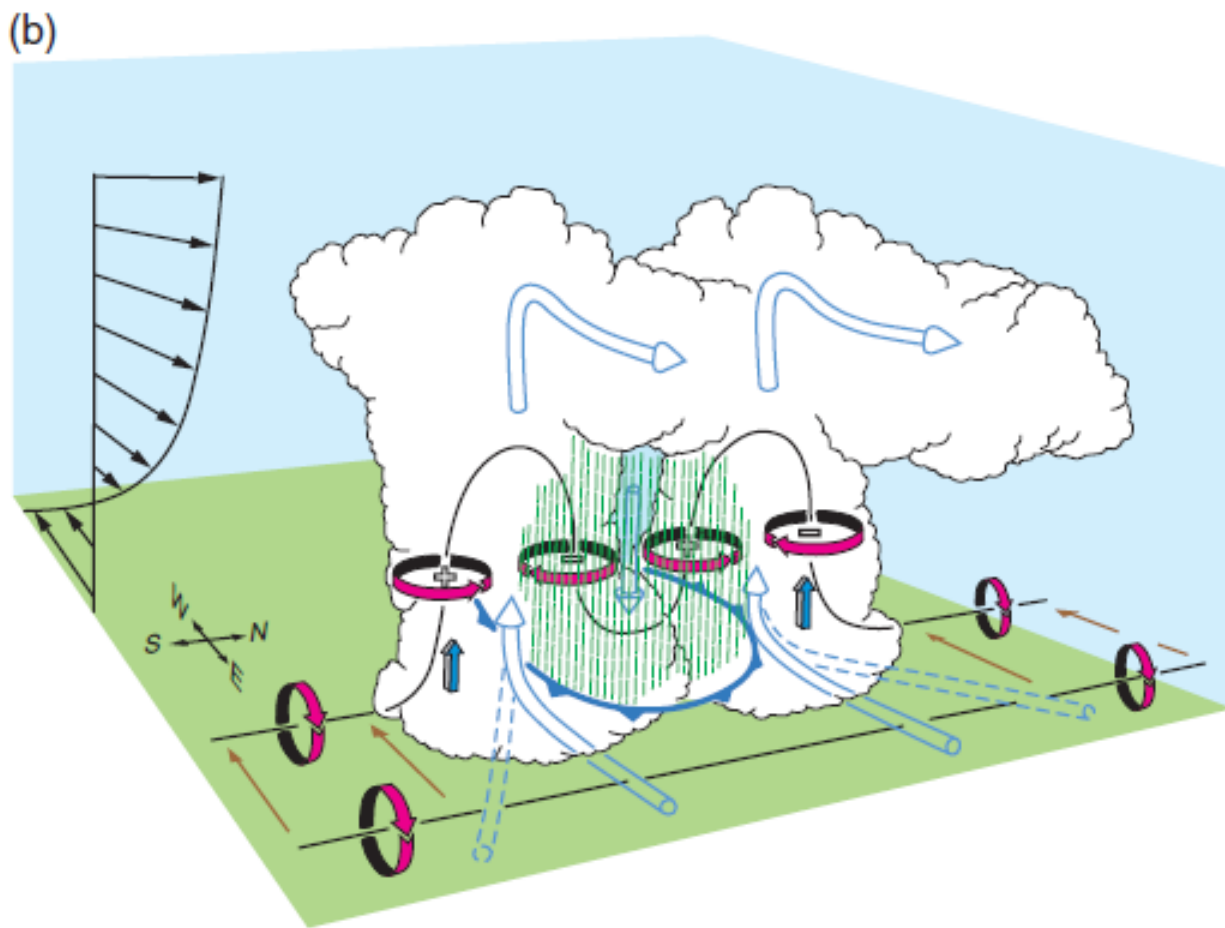


Pure crosswise vorticity
 $(\vec{v} - \vec{c}) \perp \vec{\omega}_h$



More streamwise and
 antistreamwise vorticity
 components

- 第一次分裂发生以后，虽然streamwise vorticity增大，但仍会留有一定的crosswise vorticity，只要存在crosswise vorticity，就有可能继续分裂。
- 上升流会持续不断地制造新的垂直涡度，致使风暴被持续不断地侧向传播，只要 w' 和 ζ' 不重合，这个过程就会持续，而只要有crosswise vorticity存在， w' 就永远赶不上 ζ'

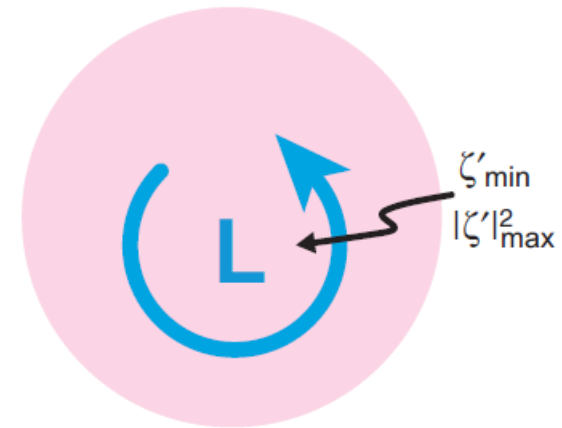
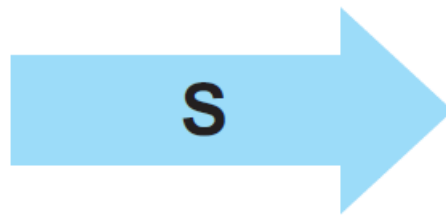


b. 环境为streamwise vorticity

w' 和 ζ' 重合，非线性强迫无法使风暴侧向传播，但是线性动力强迫可以。

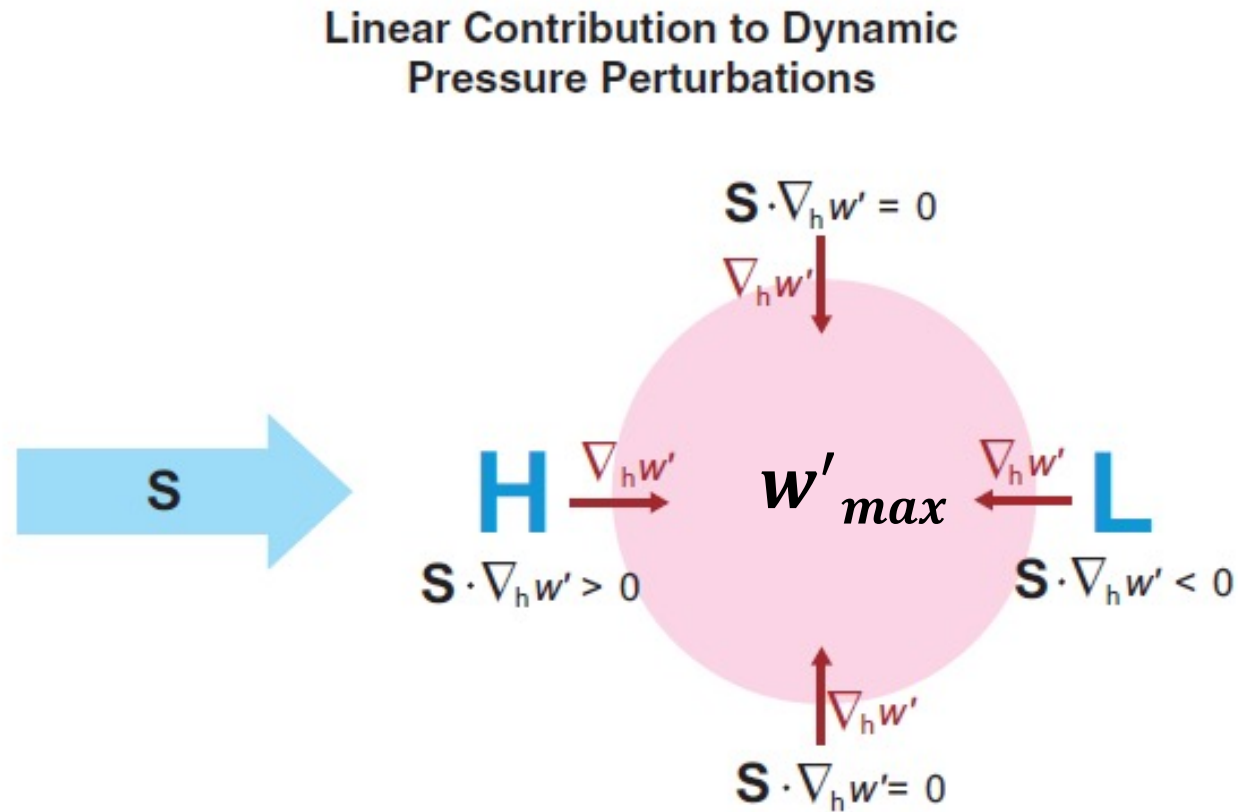
Nonlinear Contribution to Dynamic Pressure Perturbations

streamwise vorticity
(w' and ζ' highly correlated)

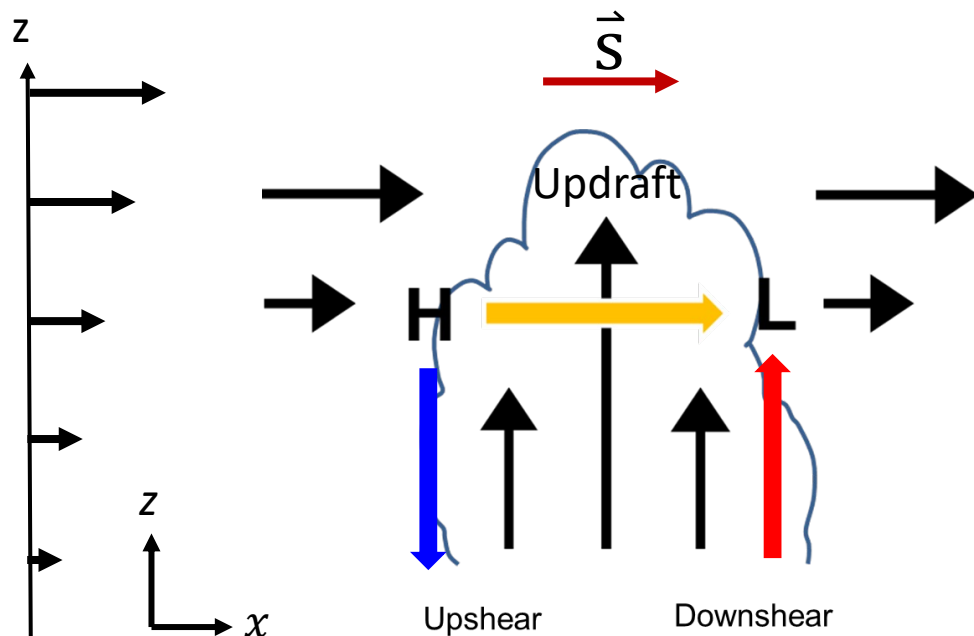


3) 线性动力强迫 $p' \propto \vec{s} \cdot \nabla_h w'$

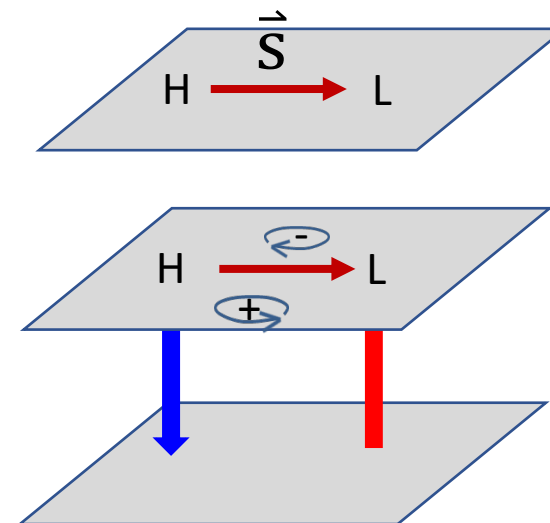
使Supercell在Veering hodograph下向平均切变矢量的右侧移动



a. Straight hodograph



$$p' \propto \frac{\partial w'}{\partial x} \frac{\partial \bar{u}}{\partial z}$$

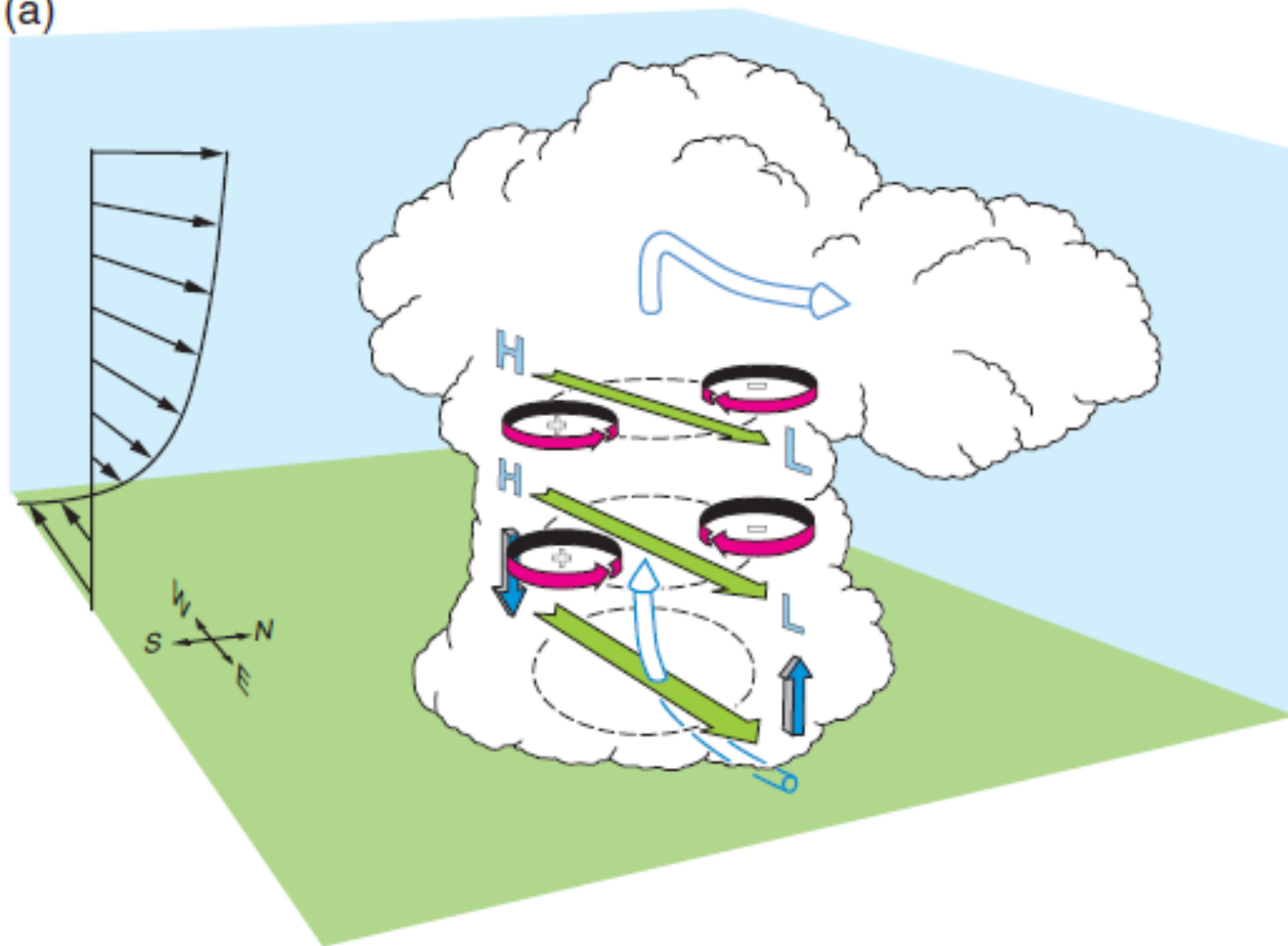


Downshear 扰动气压梯度力抬升气块到LFC

新单体生成

单体向下切变方向传播

(a)



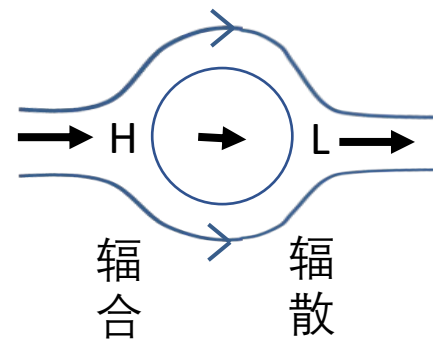
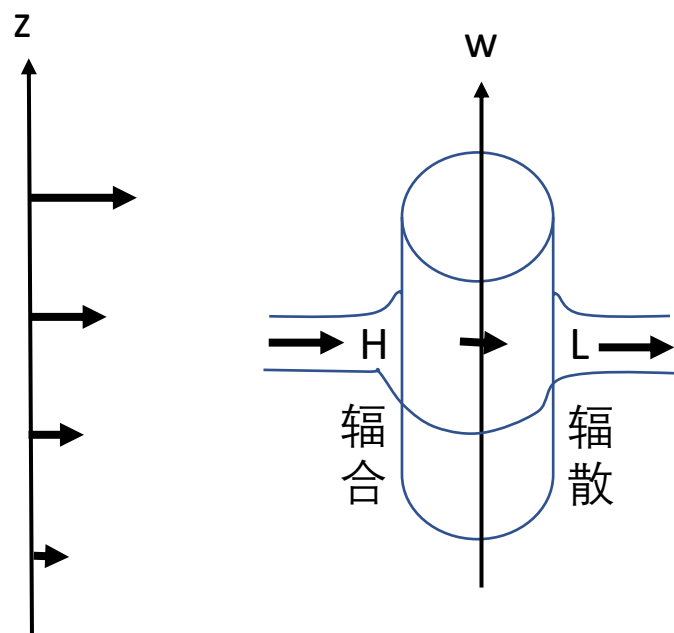
物理解释

上升气流内较小的水平动量被上传

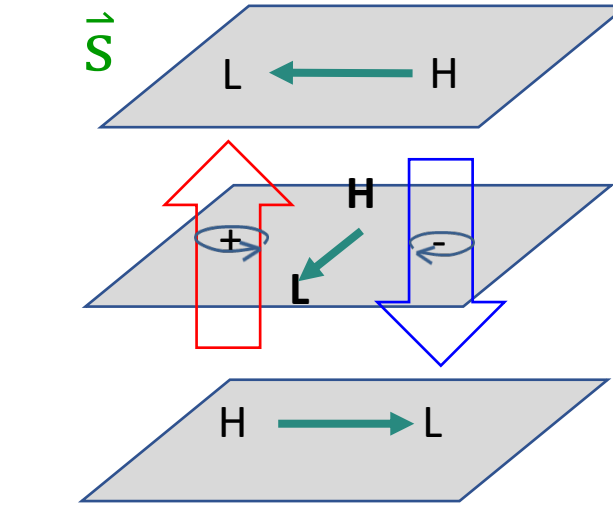
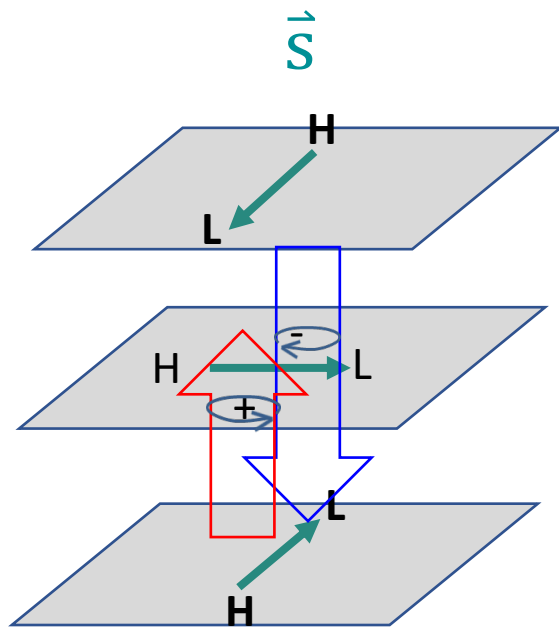
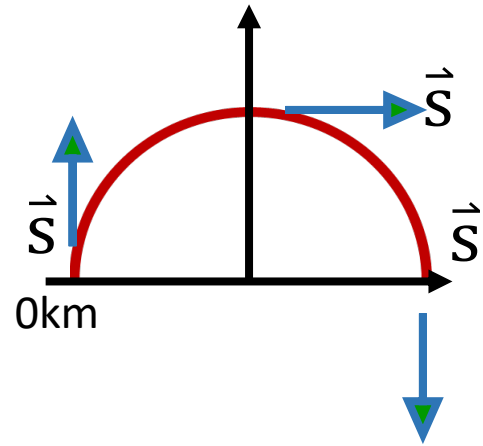
中层动量变小

上切变处辐合加压

下切变处辐散减压



b. Veering hodograph $p' \propto \vec{s} \cdot \nabla_h w'$

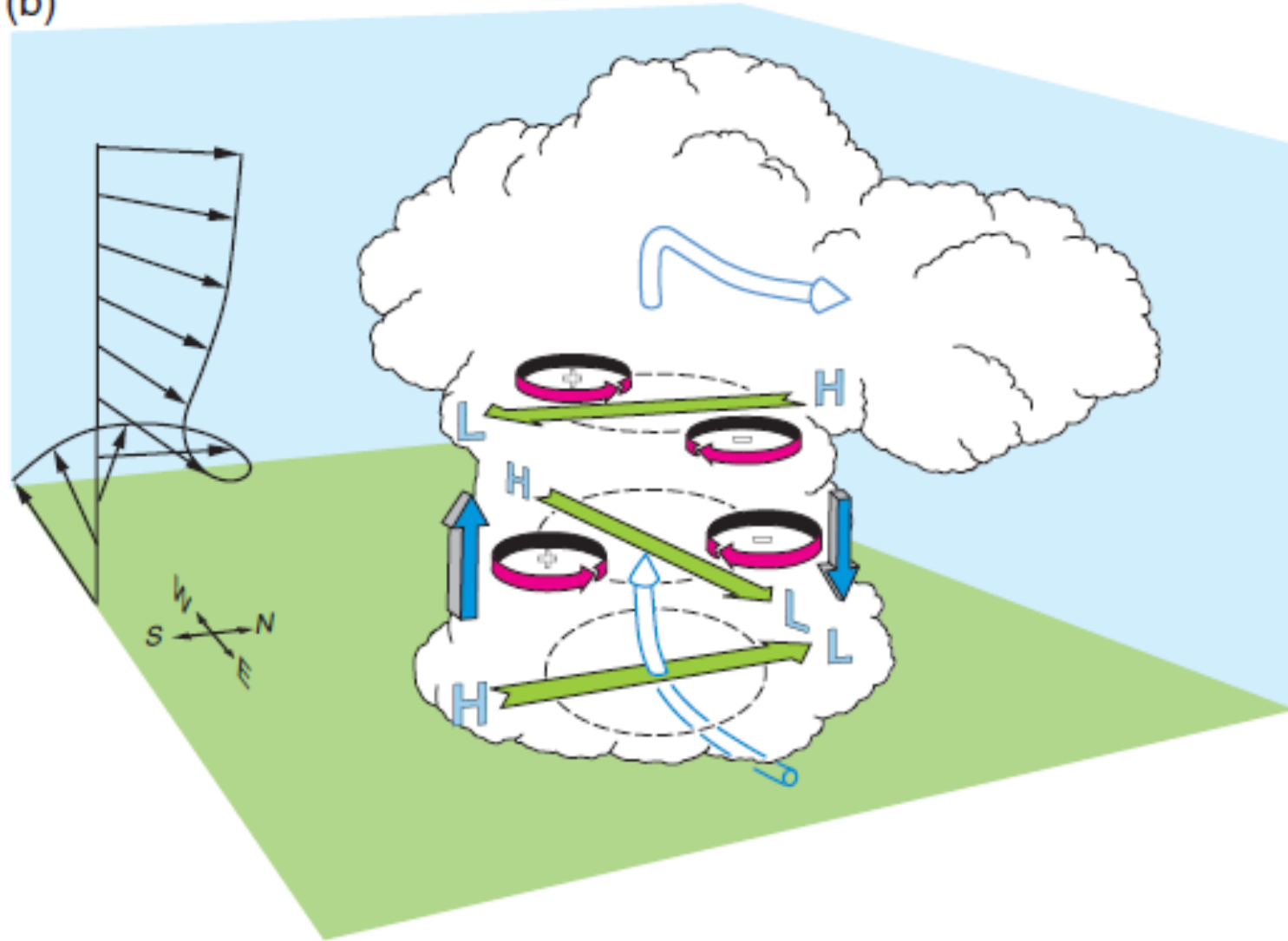


转90度指向外

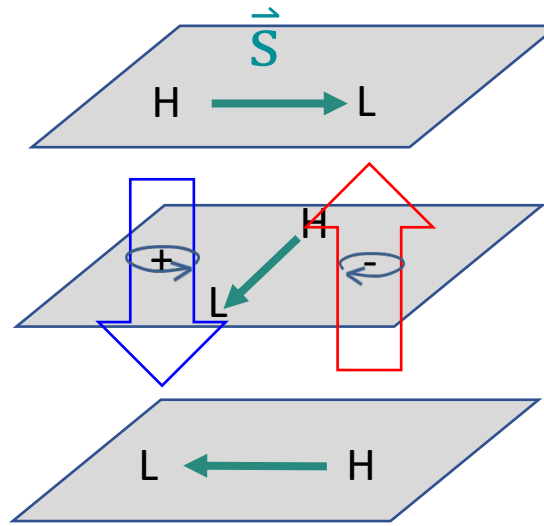
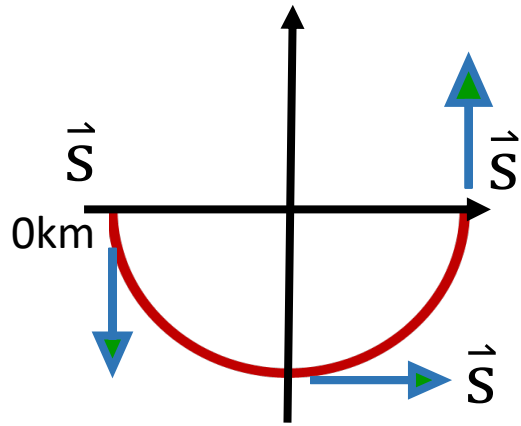
$$\frac{\partial (\vec{s} \cdot \nabla_h w')}{\partial z} \text{ 大于 Straight hodograph 情况}$$

Right mover 发展
Left mover 消亡,
可能不会常出现左
移风暴

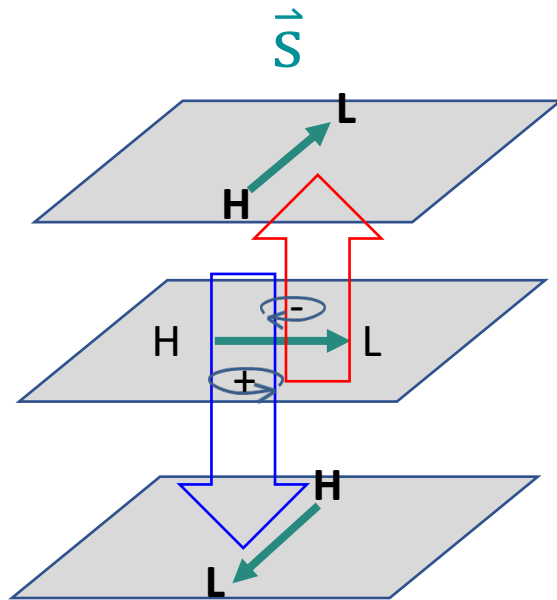
(b)



c. Backing hodograph $p' \propto \vec{s} \cdot \nabla_h w'$



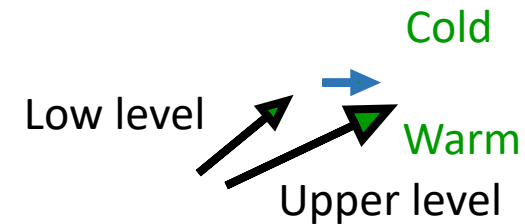
Left mover 发展
right mover
 消亡, 可能不会
 常出现右移风暴

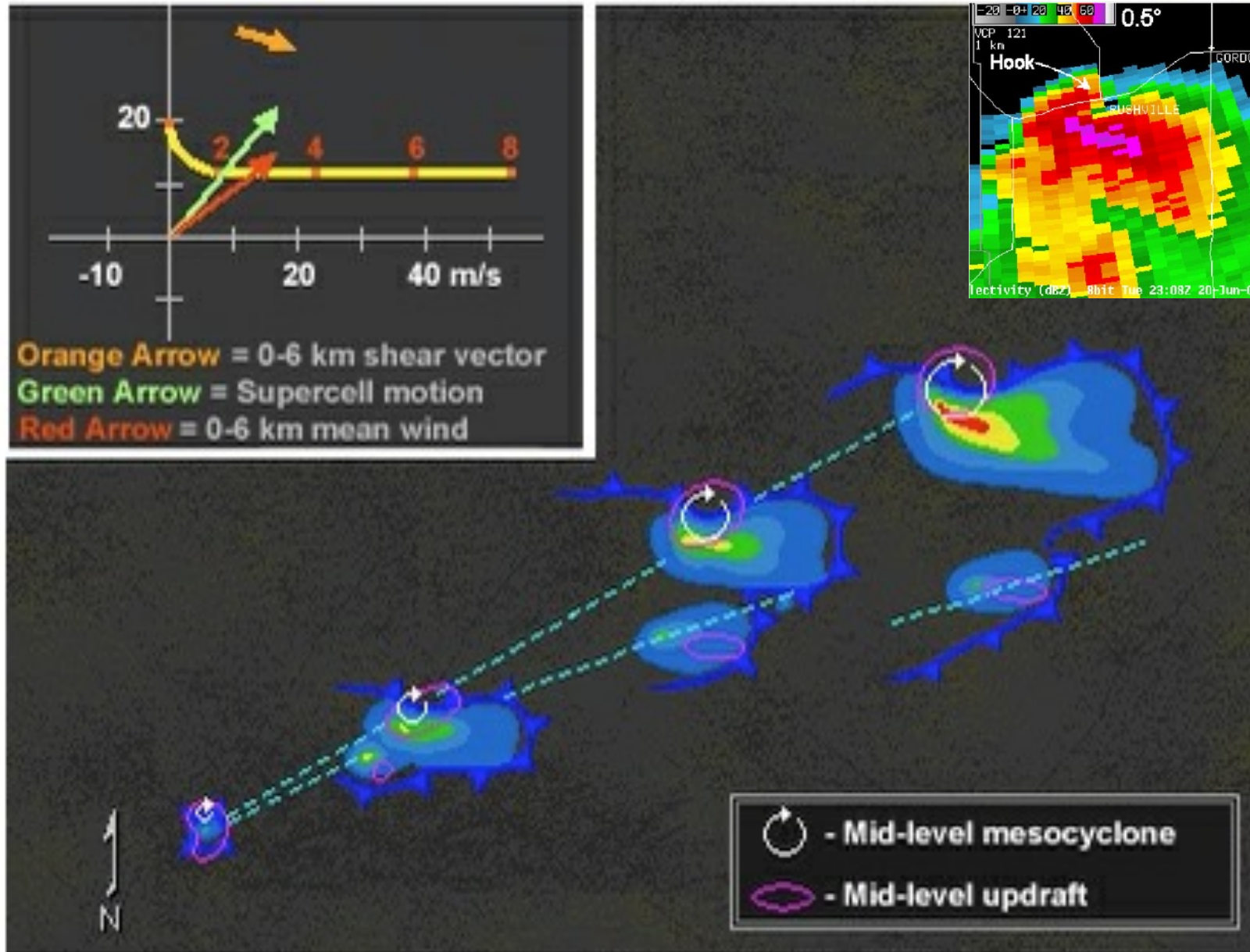


转90度指向外

Veering wind 比
Backing wind 常见

- 对流的常出现在低层暖湿气流区





Weisman and Klemp, Ray, Ed., 1986 / The COMET Program

- a. 非线性强迫有利于风暴在原上升支两侧对称发展
-Straight hodograph

- b. 线性强迫有利于Veering (Backing) 风廓线下风暴向平均切变矢量的右 (左) 侧发展
- Curved Hodograph

移动的影响因子

Mean wind, 侧向传播, Gust front

经验预报方法

a. 相对于平均风

75-80%的平均风速

25-30°右偏于平均风向

b. 相对于切变矢量(4km高度处的风与0-500m平均风之差) (Rasmussen and Blanchard,1998)

c. 相对于切变矢量(5.5-6 km平均风与0-500m平均风之差)

(Bunkers et al. 2000)

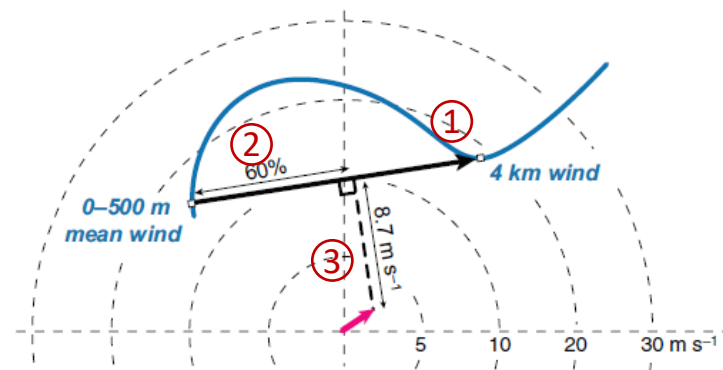


Figure 8.43 The Rasmussen and Blanchard (1998) method for forecasting supercell motion predicts a motion 8.7 m s^{-1} orthogonal to the right of a location 60% of the distance from the tail to the head of the shear vector drawn between the 0-500 m mean wind and the 4 km wind. In the hodograph, the magenta arrow indicates the predicted supercell motion.

(1) 基于数值模拟的概念模型 (Weisman and Klemp 1986)

风暴的特征主要取决于阵风锋辐合+动力扰动气压的强迫，决定于垂直风切变的大小、形状和厚度。

模式背景：适当不稳定，**CAPE=2000 J/kg**
均匀背景，**5km**之上风为常数。

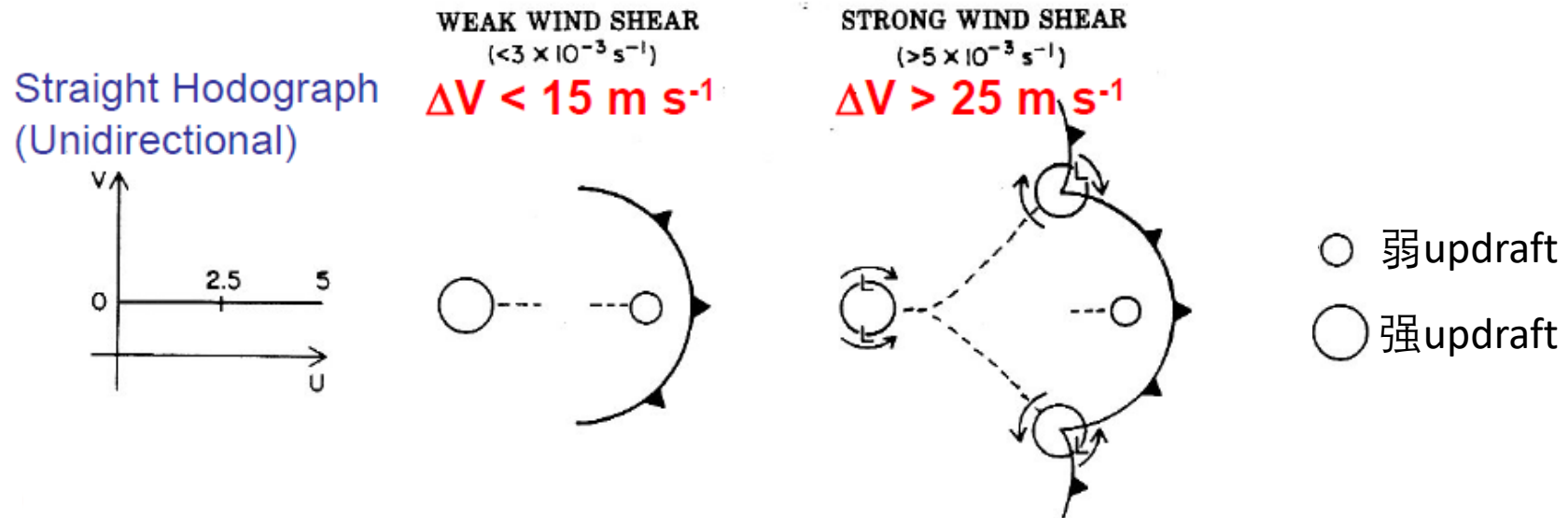
1) 单一方向切变

a. 弱切变 $< 3 \times 10^{-3} \text{s}^{-1}$

冷池在下切变方向触发后继对流

b. 强切变 $> 5 \times 10^{-3} \text{s}^{-1}$

上升支两侧低压发展，中层最强，上升支分裂为两个，分别向平均风两侧移动，右移的为气旋性，左移的为反气旋性。



2) 曲线切变 (Veering)

地面以上2km内风向顺时针变化

a. 弱切变 $< 3 \times 10^{-3} \text{s}^{-1}$

常单体在阵风锋前部和左侧不断生成

为啥左侧?

b. 强切变 $> 5 \times 10^{-3} \text{s}^{-1}$

线性扰动气压强迫导致右侧气旋性准定常风暴发展。
左侧可能会有常单体发生。

Curved (clockwise)
hodograph

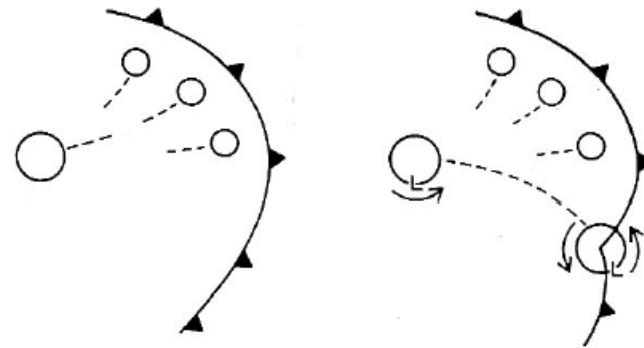
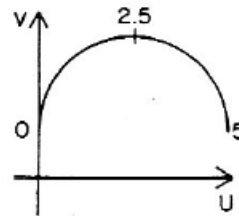


Figure 15.15. Updraft evolution in weak and strong wind shear conditions for unidirectional and clockwise-curved wind shear profiles. Hodographs on the left define the wind shear type; 0, 2.5, and 5 km levels are indicated. Large and small circles represent relatively strong and weak updrafts, respectively; the path of each updraft cell is indicated by a dotted line. Updraft structure is depicted at the early and mature phases of each storm; surface gust fronts (barbed lines) are included at the mature phase. L is the approximate position of significant middle-level mesolow features. The direction of the updraft rotation (if any) is indicated by arrows.

(2) 不同的风切变形式下的数值模拟

模式初始场：孤立轴对称热泡, $CAPE=2200 \text{ J/kg}$, 水平均匀背景

Case A: 短生命期多单体

Case B: 多单体对流线南端发展Supercell

Case C: 风暴分裂, 右侧发展

Case D: 经典的右移发展Supercell

Case E: 弱飚线 (Multicell)

Case F: 飚线 (Bow-echo)

(2) 不同的风切变形式下的数值模拟

分析设置

时次为**40、80、120min**

1.8km高度的 q_r (类似于雷达回波) **kg/kg : contour**

中层**4.6km**的上升气流 **> 5m/s: Shaded**

上升支路径: **dashed**

地面阵风锋 (**$-1^{\circ}\text{C T}'$**)

风暴**80-120min**平均移速: **arrow**

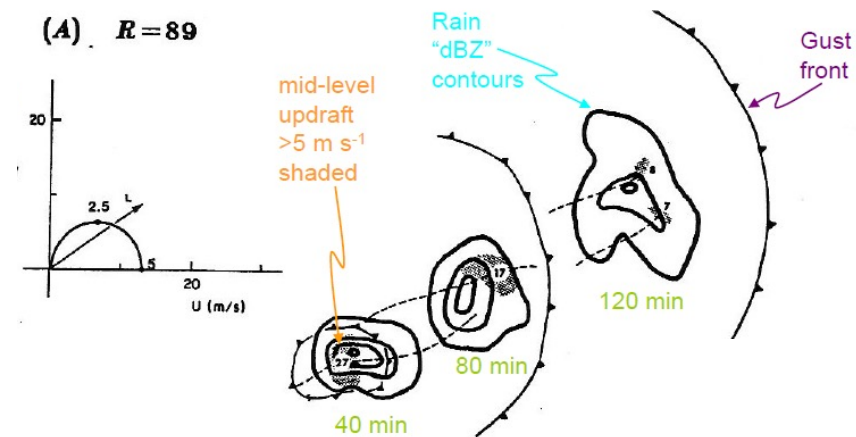
R: Bulk Richardson number

$$\text{BRN} = \text{CAPE} / (0.5 U^2)$$

$$\text{Storm relative inflow } U = V_{0-6\text{km}} - V_{0-500\text{m}}$$

CAPE 越大，下沉气流越强，预示Outflow强度。

Single cell ≥ 50 , Multi and supercell < 50



1) Case A (R=89, short-lived multicell)

High BRN , Low shear, 180° turning lowest 5 km

Warm bubble ⇒ updraft ⇒ Liquid water ⇒ Downdraft rain

⇒ Cold pool ⇒ Gust front ⇒ 新单体在前左侧生成

⇒ Gust front 最终移到风暴前面，风暴消亡。

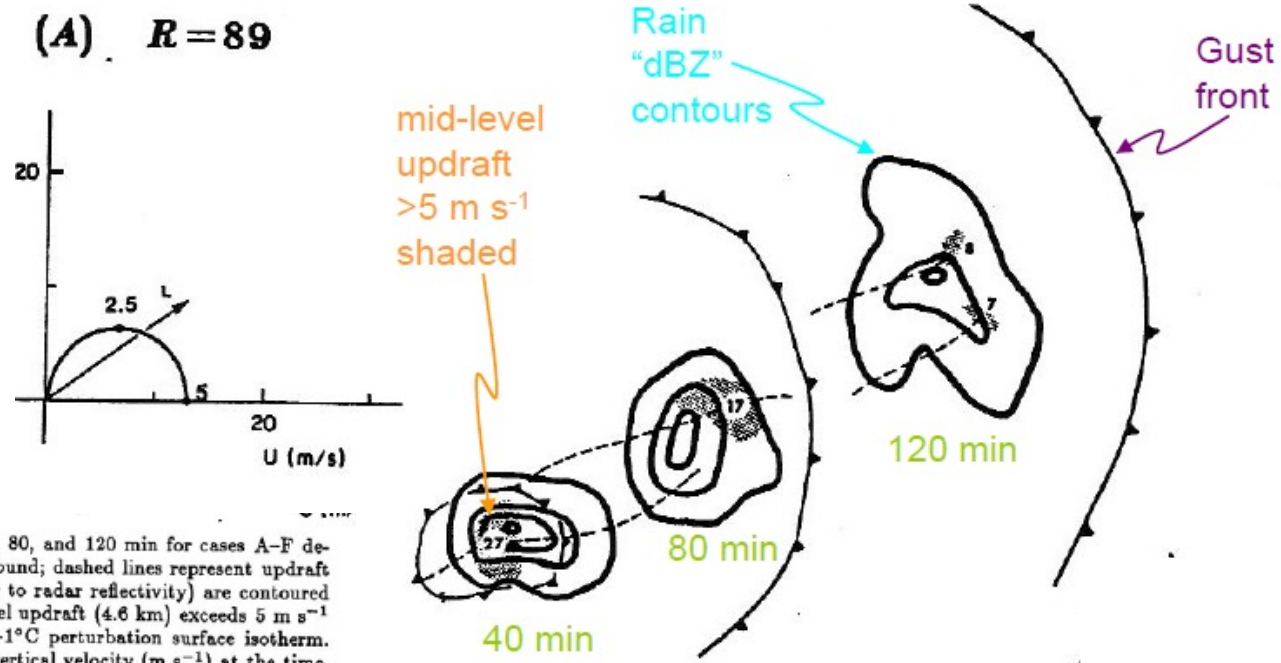
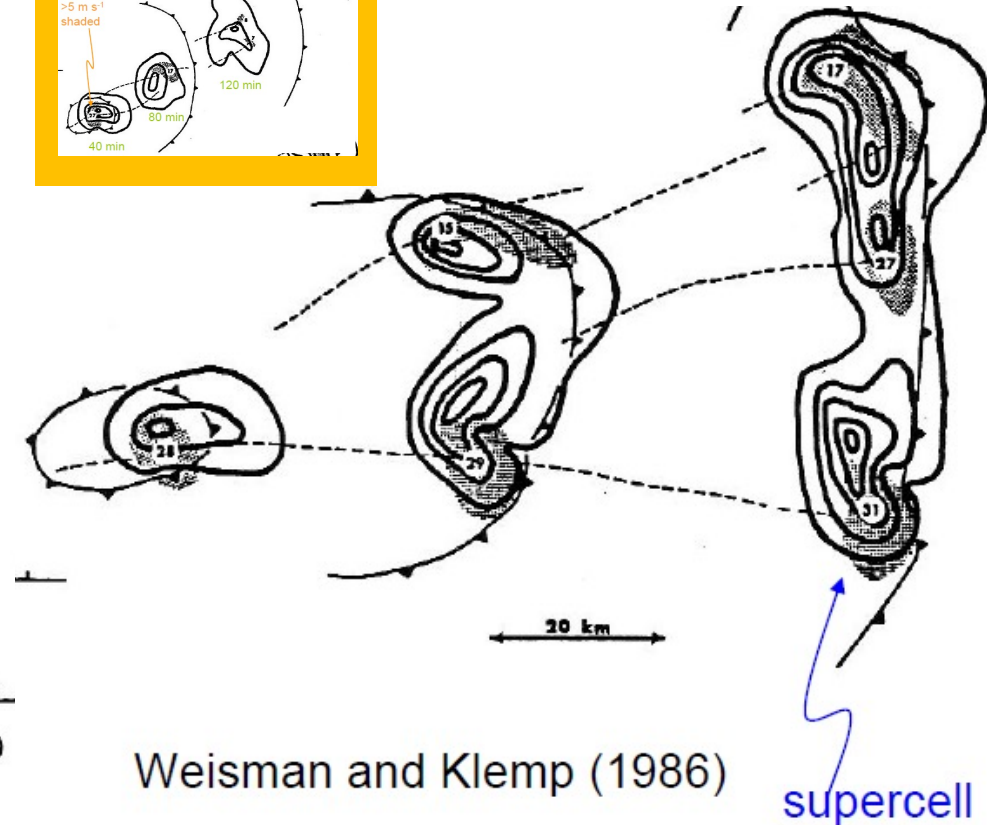
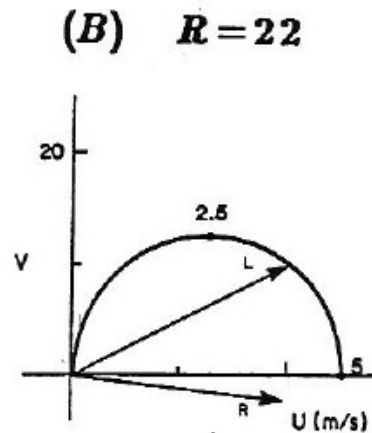
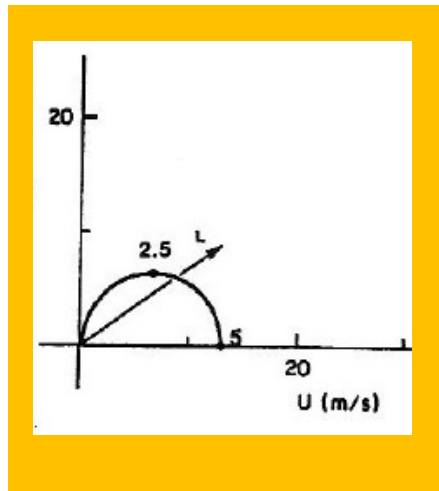
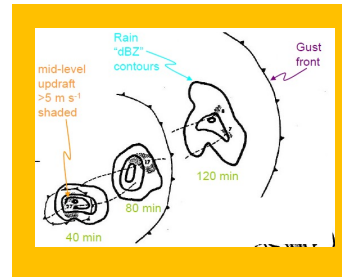


Figure 15.17. Hodograph and storm structures at 40, 80, and 120 min for cases A-F described in text. Storm positions are relative to the ground; dashed lines represent updraft cell path. Low-level (1.8 km) rainwater fields (similar to radar reflectivity) are contoured at 2 g kg^{-1} intervals. Regions in which the middle-level updraft (4.6 km) exceeds 5 m s^{-1} are shaded. Surface gust fronts are defined by the -1°C perturbation surface isotherm. Numbers at the updraft centers represent maximum vertical velocity (m s^{-1}) at the time. On hodographs, heights are labeled in km agl and arrows indicate the mean storm motion between 80 and 120 min. R = bulk Richardson number as discussed in Sec. 15.5.1. Cases A and B, multi-cell and supercell storms.

2) Case B ($R=22$, supercell on the south side of a multicell line)

- Hodograph形状同**Case A**，但大小加倍
- 较强的Veering hodograph使初始上升支右侧对流发展
- 初始的单体发展成Supercell，向平均切变矢量的右侧移动，出现hook echo
- 左侧发展一些随机的对流
- Supercell比左侧对流强
- 强切变下，gust front一直保持在上升支附近



3) Case C ($R=15$, Right-flank supercell split from weaker left flank storm)

Curved Hodograph

0-2km shear 大小同 Case B,
2-5km 为一条线

- 初始风暴右移，形成 Supercell，左侧出现不定常降水，没出现 hook echo，上升气流较强。
- 高层切变较小的弯曲度使得左侧风暴与右侧风暴脱离
- 表现为两个逐渐远离彼此的风暴，右侧的较强。

Straight Hodograph

初始风暴分裂为两个对称的左移和右移超级单体。

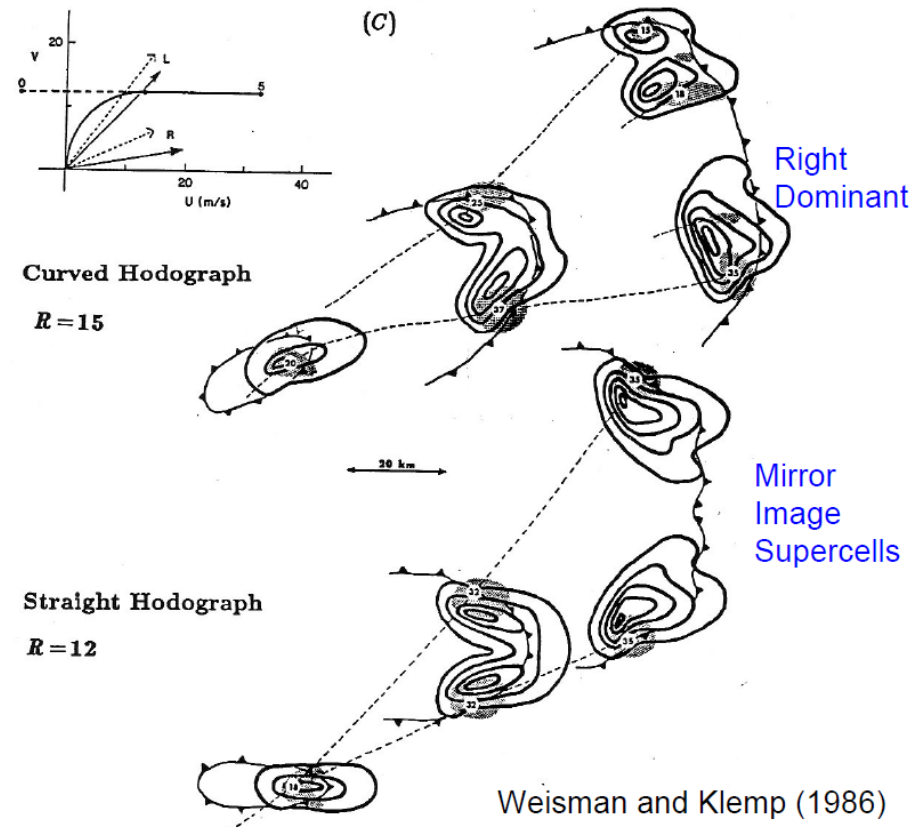
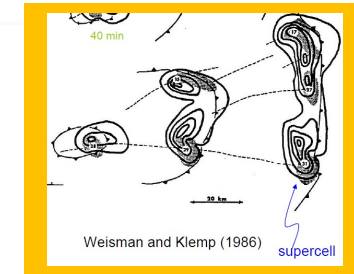
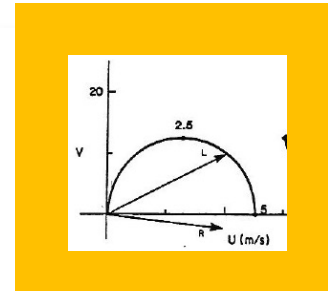
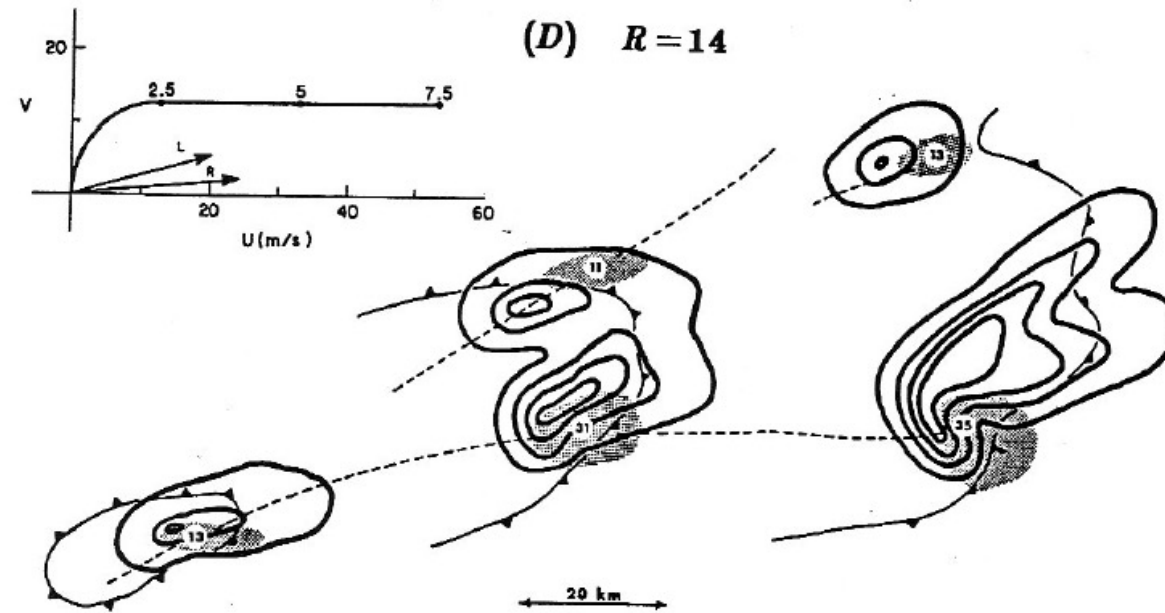
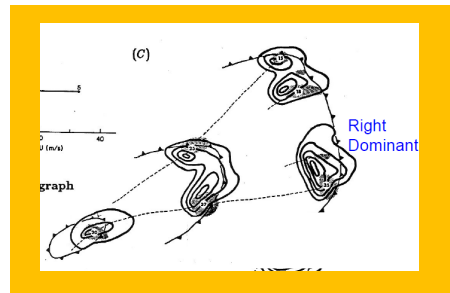
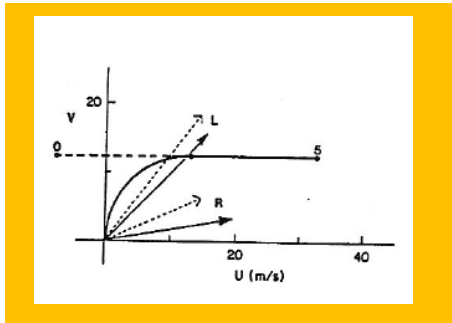


Figure 15.17. Continued. Case C, splitting supercell storms.

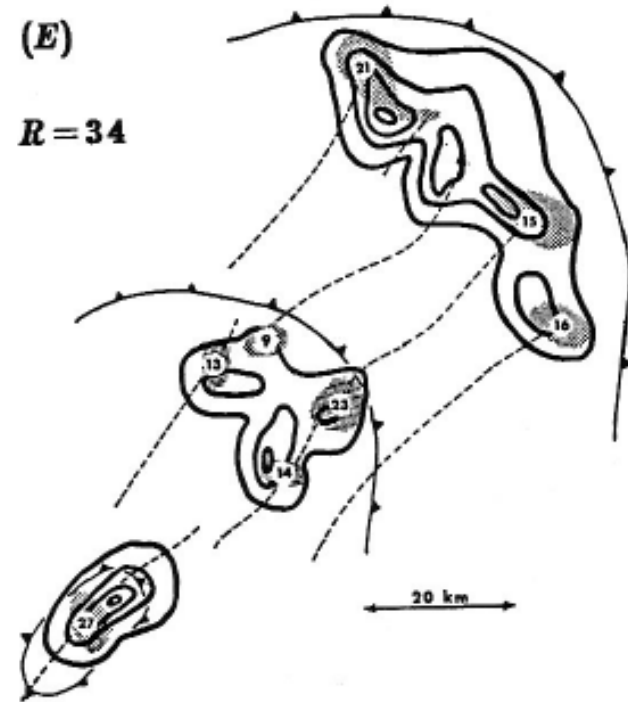
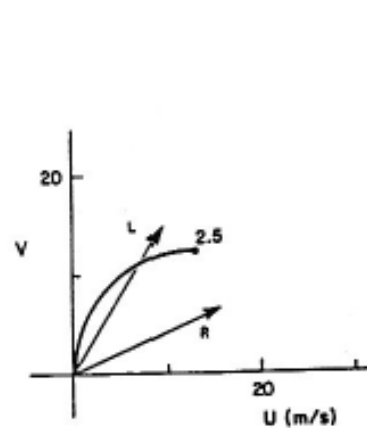
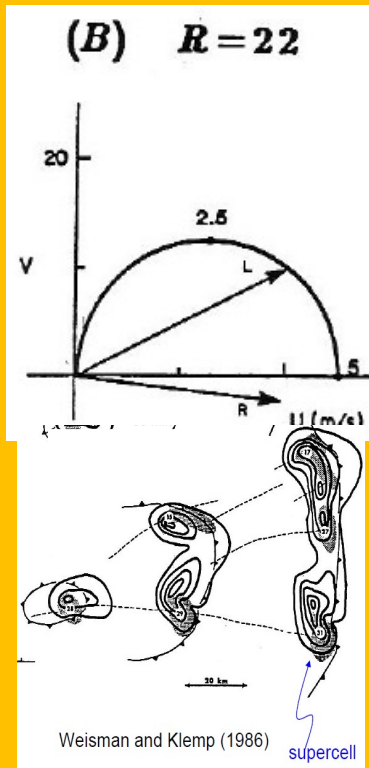
4) Case D (R=14, Right-flank supercell)

- 同Case C, 但直线部分延伸到7.5 km
- 初始风暴发展为右移Supercell
- 看上去像Classic supercell, hook echo, mesocyclonic updraft, FFD
- 左侧对流很弱, 120min 时已基本消失



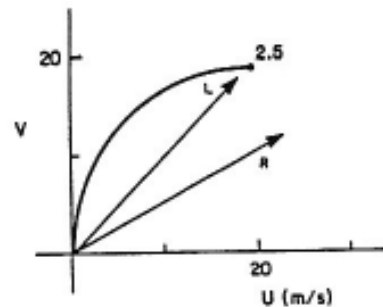
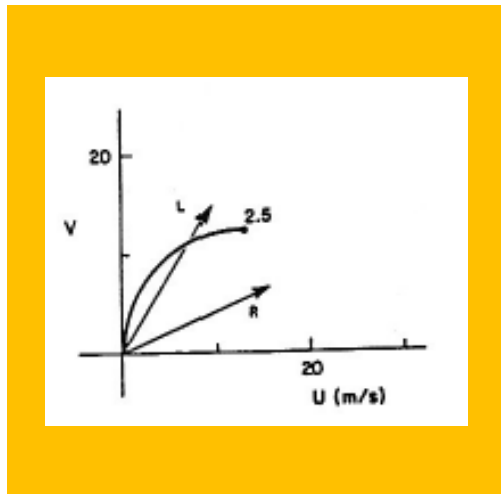
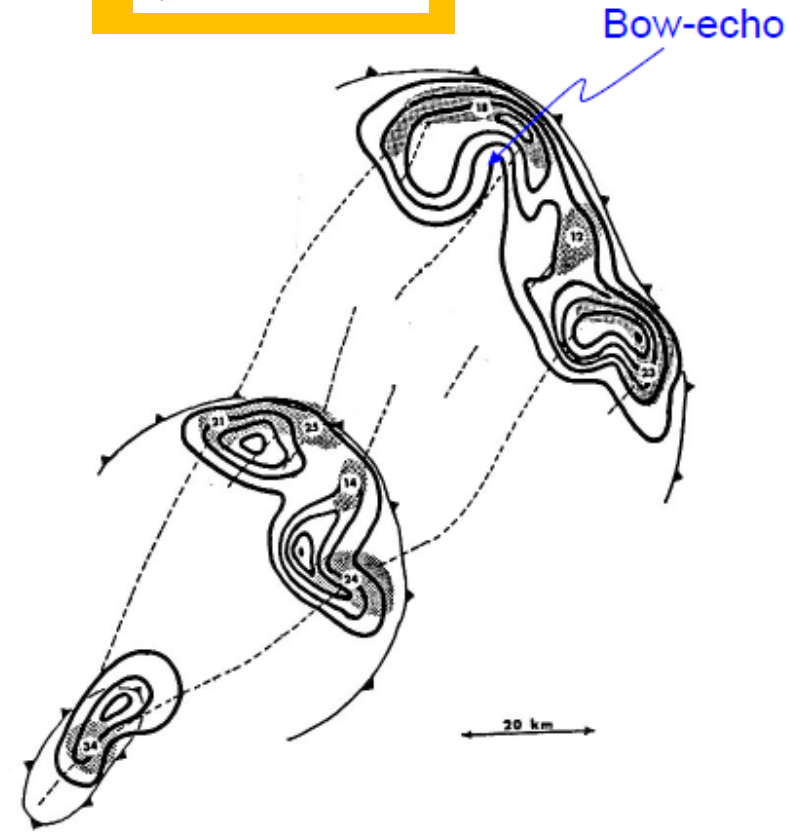
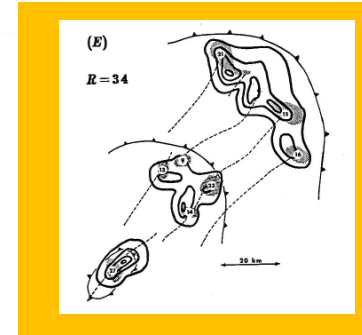
5) Case E ($R=34$, weak squall line)

- Shear类似于**Case B**，但在2.5km 处截断
 - 较小的Curvature和较浅的切变
- 中等强度的浅层切变产生的扰动气压强迫不足以维持Supercell
- 不定常上升气流在下切变方向生成，形成多单体
- Gust front移动稍快于对流。



6) Case F (R=20, squall line with bow echo)

- Shear同CaseE, 但大小增加50%
- 切变较强, 足以产生右侧的稳态上升气流, 但Supercell偏弱 (相对深层切变)
- 可发展出下击暴流, Bow echo
- 80 min 出现Spear head
- 120 min 北部出现旋转型Comma状的squall line, 地面风达到35-40 m/s。



(3) 天气



- 非定常风暴可能造成严重灾害 (High CAPE)
- 对于相同的CAPE, Supercell比多单体灾害重

(4) 小结



影响对流风暴组织的主要环境因子：

- CAPE
- Cold pool 出流特征
- 垂直扰动气压梯度力

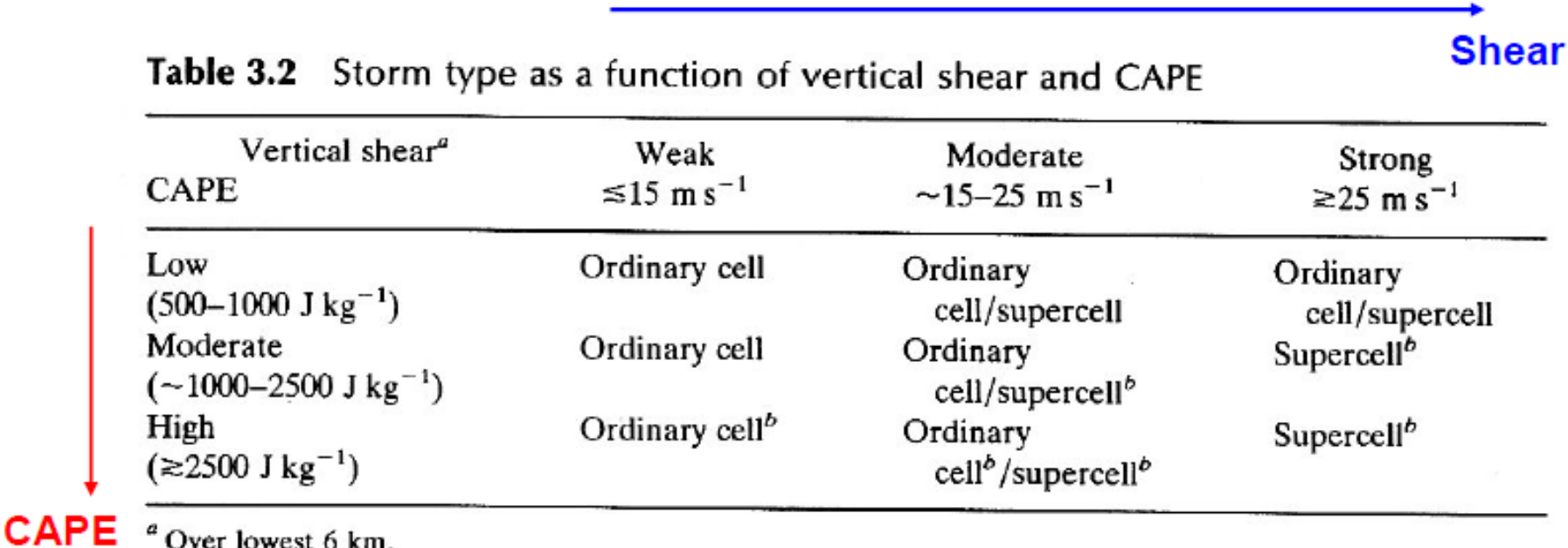
Weak shear
CAPE \Rightarrow Cold pool 无法连续触发对流 \Rightarrow Ordinary cell

Moderate shear
Low-moderate CAPE \Rightarrow Cold pool 不断触发常规单体 \Rightarrow Multicell

High shear
CAPE \Rightarrow 垂直扰动气压梯度力 \Rightarrow Supercell

Storm type as a function of vertical shear and CAPE

Table 3.2 Storm type as a function of vertical shear and CAPE



Vertical shear ^a CAPE	Weak $\approx 15 \text{ m s}^{-1}$	Moderate $\sim 15\text{--}25 \text{ m s}^{-1}$	Strong $\geq 25 \text{ m s}^{-1}$
Low (500–1000 J kg ⁻¹)	Ordinary cell	Ordinary cell/supercell	Ordinary cell/supercell
Moderate (~1000–2500 J kg ⁻¹)	Ordinary cell	Ordinary cell/supercell ^b	Supercell ^b
High ($\geq 2500 \text{ J kg}^{-1}$)	Ordinary cell ^b	Ordinary cell ^b /supercell ^b	Supercell ^b

^a Over lowest 6 km.

^b Storms in which severe weather is likely. Vertical shear is measured by the length of the hodograph of the environmental winds from the surface to 6 km AGL (small-scale curves and loops are not counted). Supercells can occur even in environments of low CAPE if there is low CIN and if the environment is so moist that entrainment of environmental air does not weaken the updraft significantly. Severe weather is likely in storms produced in an environment of moderate–high CAPE regardless of storm type because the updrafts can be strong (based upon numerical simulations by M. Weisman, NCAR).

Bluestein (1993)

Storm type as a function of Bulk Richardson Number (R).

354

WEISMAN and KLEMP

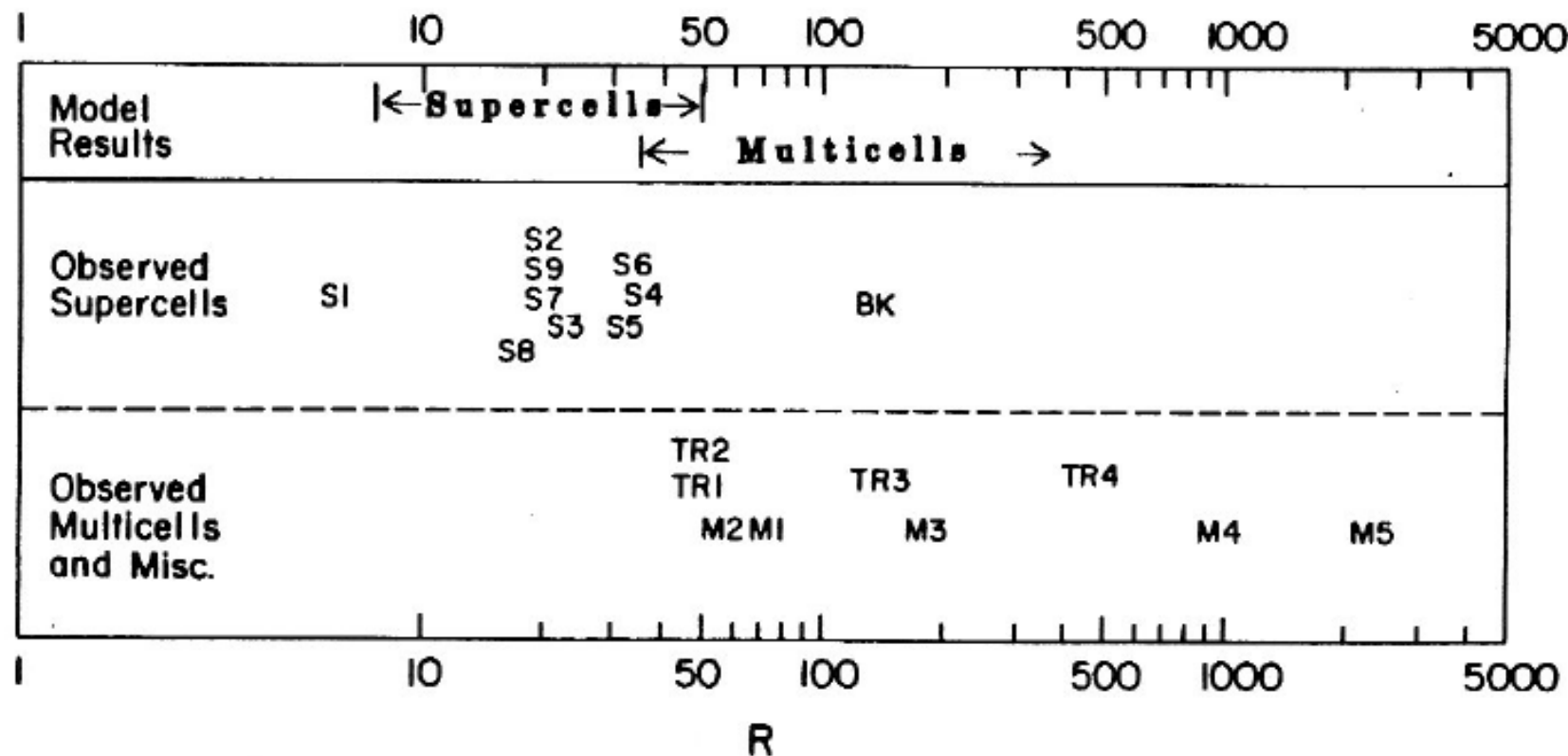


Figure 15.18. Richardson number R as calculated for a series of documented storms. Model results are summarized at the top of the figure. S1, S2, ..., S9 represent supercell storms; M1, M2, ..., M5 represent multicell storms; TR1, TR2, ..., TR4 represent tropical cases. (Adapted from Weisman and Klemp, 1982.)

Weisman and Klemp 1982